Fall 2021

Characterization of a Novel Fe-S Cluster Transfer Pathway Between GRX4 and Sufa in *Escherichia Coli*

Enis Sanchez

CHARACTERIZATION OF A NOVEL FE-S CLUSTER TRANSFER PATHWAY BETWEEN GRX4 AND SUFA IN *ESCHERICHIA COLI*

by

Enis Sanchez

Artium Baccalaureatus
College of Charleston, 2016

Bachelor of Science
College of Charleston, 2016

Submitted in Partial Fulfillment of the Requirements

For the Degree of Master of Science in

Chemistry

College of Arts and Sciences

University of South Carolina

2021

Accepted by:

F. Wayne Outten, Director of Thesis

Vitaly Rassolov, Reader

Tracey L. Weldon, Interim Vice Provost and Dean of the Graduate School

ABSTRACT

Biogenesis of iron-sulfur (Fe-S) clusters is an essential process in living organisms due to the critical role of Fe-S cluster proteins in a myriad of cellular functions. During the assembly of Fe-S clusters, multi-protein complexes are used to drive the mobilization and protection of reactive sulfur and iron intermediates, regulate assembly of various Fe-S clusters on an ATPase-dependent, multi-protein scaffold, and target nascent clusters to their downstream protein targets. In each of the Fe-S cluster biogenesis steps, specific protein-protein interactions (PPIs) are required for proper function of the assembly pathway. The target pathway is the sulfur formation (Suf) pathway for Fe-S cluster assembly found in bacteria and archaea. In *Escherichia coli*, the Suf pathway functions as an emergency pathway under conditions of iron limitation or oxidative stress. In other pathogenic bacteria, such as *Mycobacterium tuberculosis* and *Enterococcus faecalis*, the Suf pathway is the sole source for Fe-S clusters. The goal of this research is to characterize PPIs critical for bacterial Fe-S cluster assembly, which could act as a potential target for the development of novel antibacterial compounds to disrupt those interactions. Important PPIs between the Suf pathway and additional upstream and downstream cluster carrier proteins provide biologically relevant targeting functions and the ability for "crosstalk" between cluster assembly pathways. Genetic and biochemical studies suggest that *in vivo* Fe-S cluster trafficking utilizes complex mechanisms. Herein, we characterize cluster trafficking interactions between SufA and the upstream Fe-S cluster trafficking protein,

Grx4. The percentage and rate of cluster transfer suggests that Grx4 may transfer its cluster to SufA *in vivo*, as a unidirectional process.

TABLE OF CONTENTS

LIST OF FIGURES

LIST OF ABBREVIATIONS

BSA ..... Bovine Serum Albumin

βME ..... β-mercaptoethanol

C or Cys ..... Cysteine

$CaCl_2$ ..... Calcium Chloride

CD ..... Circular Dichroism

DEAE ..... Diethylaminoethanol

DTT ..... Dithiothreitol

E. coli ..... *Escherichia coli*

EDTA ..... Ethylenediaminetetraacetic acid

ESI ..... Electrospray Ionization

Fe-S ..... Iron-Sulfur

FF ..... Fast Flow

FPLC ..... Fast Protein Liquid Chromatography

Fur ..... Ferric Uptake Regulator

Grx ..... Glutaredoxin

GSH ..... Glutathione

H_2O_2 ..... Hydrogen Peroxide

IPTG ..... Isopropyl-β-D-thiogalactoside

Isc ..... Iron Sulfur Cluster

kDa ..... kiloDalton

LB ..... Lennox Broth

LC .....Liquid Chromatography

MQ .....MilliQ

MS.....Mass Spectrometry

NaCl ..... Sodium Chloride

NH_4SO_4 .....Ammonium Sulfate

Nif .....Nitrogen Fixation

OD..... Optical Density

PDB.....Protein Data Bank

PLP..... Pyridoxal 5-phosphate

PMSF .....Phenylmethylsulfonyl Fluoride

ROS.....Reactive Oxygen Species

SDS ..... Sodium Dodecyl Sulfate

PAGE .....Polyacrylamide Gel Electrophoresis

Suf.....Sulfur formation

TCA.....Tricarboxylic Acid

TCEP.....Tris(2-carboxyethyl)phosphine

TFA .....Trifluoroacetic Acid

Tris ..... Tris(hydroxymethyl)aminomethane

UV-vis.....Ultraviolet-Visible Spectroscopy

CHAPTER 1
INTRODUCTION

Iron

Transition metal bioavailability has substantially varied in abundance over the course of geographic and evolutionary history, and over time, this variation in availability substantially influenced the metabolic strategies and biological evolution of life.[1-3] One of the metals that shaped the ecologic development of earth is iron, the fourth most abundant element in the crust of planet earth. Iron is an essential trace metal that can be found in virtually all organisms, from bacteria to humans, as it participates in a wide variety of metabolic processes, including oxygen transport, deoxyribonucleic acid (DNA) synthesis, and electron transport.[4] Iron is a first-row transition metal with incompletely filled *d* orbitals with the potential form compounds in a wide range oxidation states, ranging from Fe^{2-} to Fe^{7+}.[5,6] However, at physiological pH, the two most abundant and biologically relevant forms of iron are ferric (Fe^{3+}) and ferrous (Fe^{2+}). Around 2.5 billion years ago, atmospheric oxygen levels began rising, changing iron bioavailability from the Fe^{2+} (ferrous) state to the oxidized Fe^{3+} (ferric) state, which caused microorganisms to evolve and develop new ways to metabolize iron and oxygen.[1,2,7] While Fe^{3+} is more plentiful and less toxic to organisms, it lacks solubility under aerobic conditions, resulting in the evolution of siderophores (iron carriers) and iron-storage proteins.[8] On the other hand, Fe^{2+} has greater solubility, but has a propensity to generate harmful reactive oxygen species (ROS), such as highly toxic hydroxyl free radicals (OH•), via a process known as the

Fenton reaction. [9] Iron acts as a redox catalyst of the catalase reaction, by which hydrogen peroxide (H_2O_2) is decomposed to water and oxygen, through three reactions known collectively as the Haber-Weiss cycle (Figure 1.1). [9,10] Hydroxyl radicals, which cannot be detoxified by an enzymatic reaction, inevitably cause oxidative stress, among other detrimental effects, such as DNA mutations, lipid peroxidation, and amino acid conversions.[11,12] To achieve effective iron homeostasis, organisms must balance their need to efficiently scavenge iron from their environment to maintain adequate intracellular reserves, while carefully managing cellular free iron levels to protect against iron-induced toxicity.[8] Fe atoms are associated with many proteins as part of hemes, mono- or di-iron non-heme centers, or iron–sulfur (Fe–S) clusters.[13]

Iron-Sulfur Clusters and their Functions

Fe-S clusters rank among the most ancient, ubiquitous, and versatile classes of metal cofactors, found in over 200 distinct types of proteins and enzymes from all kingdoms of life. [14-16] The base structure of Fe-S clusters consist of iron in the Fe^{2+} or Fe^{3+} oxidation states bound to sulfide (S^{2-}) and can form a variety of configurations, including [2Fe-2S], [3Fe-4S], or [4Fe-4S] clusters.[17] Larger, more complex Fe-S structures also occur in nature, such as the [7Fe-8S] P-cluster and the FeMo cofactor, composed of [Mo-3Fe-3S] and [4Fe-3S] clusters, of the nitrogenase complex.[18] While different types of Fe-S exist in nature, the two most abundant forms are the rhombic [2Fe-2S] and the cubic [4Fe-4S] types, generated via the fusion of two [2Fe-2S] clusters. [19,20] Generally, the iron ion is held in place via the thiolate sulfur of cysteine residues, with a tetrahedral S coordination at each iron site, but other amino acids such as serine, histidine, and aspartate have been shown to act as ligands.[21]

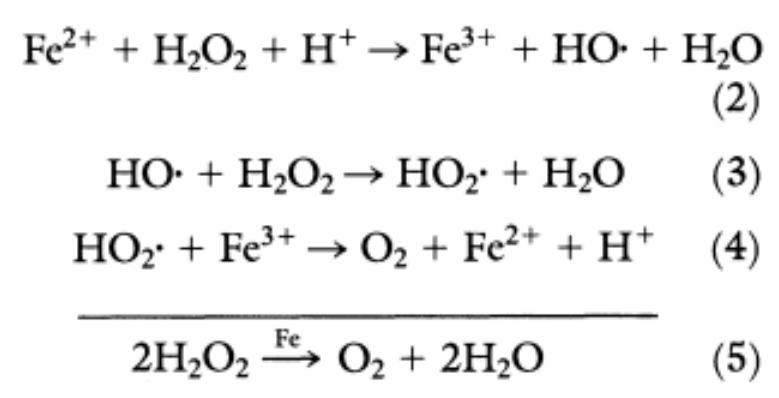

Figure 1.1. Fenton and Haber – Weiss reaction.[9]

Due to their ability to delocalize electron density over both Fe and S atoms, they are ideally suited for mediating biological electron transport.[21] Due to their chemical versatility, iron sulfur (Fe-S) centers are utilized for diverse biological functions including electron transfer, substrate activation, and regulation of gene expression.[22] Iron-sulfur (Fe-S) clusters are metal cofactors required for essential biological pathways, including respiration, photosynthesis, nitrogen fixation, and DNA repair. [13,17] In bacteria, Fe-S clusters can detect different types of environmental stimuli, using distinct sensing mechanisms, to regulate gene expression. For example, the SoxR protein senses oxidative stress via oxidation of the [2Fe-2S] cluster and thereby stimulates transcriptional expression of SoxS, which is responsible for activating the transcription of numerous other enzymes in the oxidative stress response. [23] Despite their importance, Fe-S clusters can be sensitive to oxidation by reactive oxygen, nitrogen species, and to disruption by thiophilic metals, such as copper and cobalt, presenting challenges for cluster synthesis and binding to proteins.[24,25] As such, the biosynthesis and trafficking of Fe−S clusters to the hundreds of target Fe−S proteins is achieved through highly conserved biosynthetic machinery, and not surprisingly, defects in these Fe−S assembly pathways are associated with numerous human diseases.[26-28] Despite the importance of these cofactors, unanswered questions remain regarding the biosynthesis and insertion of Fe−S clusters into target proteins.

Iron-Sulfur Cluster Biogenesis Pathways

As both free iron and sulfide are highly reactive and toxic *in vivo*, assembly of such clusters and maturation of iron-sulfur cluster proteins does not occur spontaneously. Instead, Fe-S cluster assembly requires carefully coordinated biosynthetic pathways in living cells that utilize a donation of sulfide as a bridging ligand for iron ions. These

pathways can be relatively simple as evidenced in evolutionarily ancient anaerobic organisms or highly complex such as in multicompartmental eukaryotic cells.[29] However, there are core components of Fe-S cluster biogenesis pathways found in nearly all organisms studied to date. The first step in Fe-S cluster biogenesis is the assembly of iron and sulfur on the scaffold protein. Sulfur is provided by a cysteine desulfurase complex, which converts L-cysteine to alanine through a persulfide intermediate.[30] The origin of iron is still unclear.[31] These two components, iron and sulfide, first combine on a protein that serves as a scaffold for nascent cluster assembly. Due to the lability of the scaffold-bound cluster, it can be transferred to an appropriate apo-form of a metalloprotein, either directly or using a series of carrier proteins that mediate trafficking and targeting of the mature Fe–S proteins.[32] Multiple Fe-S cluster assembly pathways are present in bacteria to carry out basal cluster assembly, stress-responsive cluster assembly, and enzyme-specific cluster assembly. Three major biosynthesis pathways have been identified to date: the Isc (*i*ron *s*ulfur *c*luster) system, the Suf (*su*lfur *f*ormation) system, and the Nif (*ni*trogen *f*ixation) system (Figure 1.2).[33] Initially discovered in azototrophic (nitrogen-fixing) bacteria, the Nif pathway operates in association with the maturation of Fe-S containing nitrogenase enzymes.[34] In our model organism *E. coli*, Fe-S cluster biogenesis is carried out by the Isc (*iscRSUA-hscBA-fdx-iscX*) and Suf (*sufABCDSE*) pathways.

The Isc Pathway

Under normal cellular conditions, the following genes of the isc operon are induced, serving as the primary Fe-S "housekeeping" pathway: *iscR, iscS, iscU, iscA, hscB, hscA, fdx,* and *IscX*. These eight key proteins of the Isc pathway are responsible for the synthesis of Fe-S clusters in *E. coli*, and higher eukaryotes have evolved orthologues of iron-sulfur

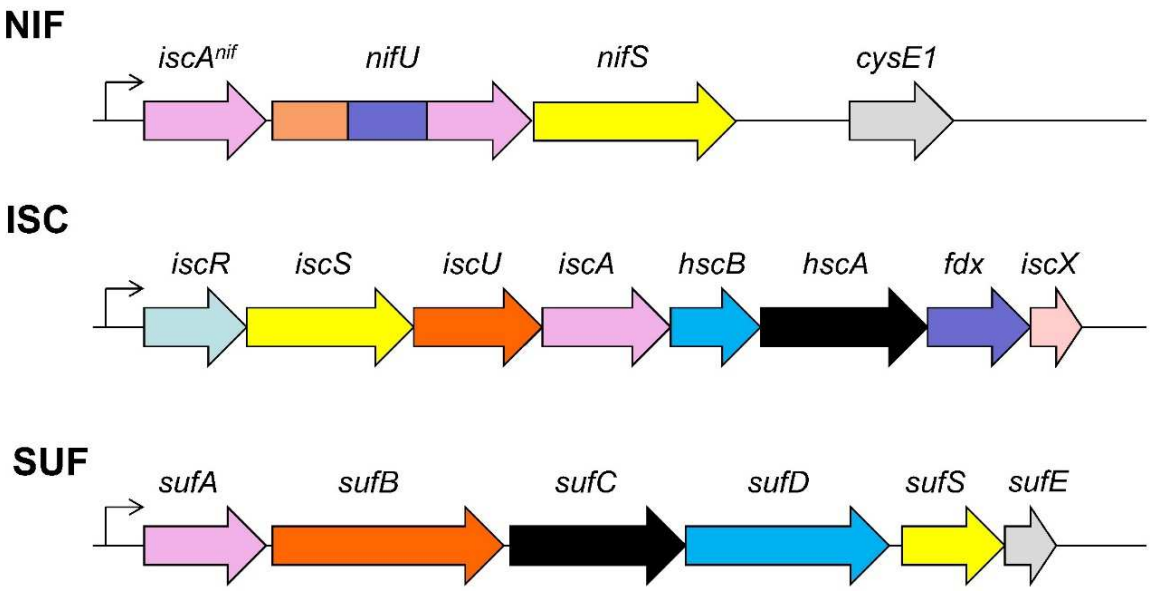

Figure 1.2. Various systems involved in Fe/S assembly in bacteria and comparison of their genetic organization in operons: NIF, ISC and SUF.[33] Genes or regions having homologous sequences or similar functions between the three systems are color-coded. Different colors within *nifU* indicate different domains within this modular protein.

cluster assembly proteins for iron-sulfur cluster biosynthesis within mitochondria.[35] While extensive biochemical and genetic studies have elucidated well-defined roles for the core proteins IscS, IscU, and IscA, such roles have not been determined for the HscB, HscA, Fdx, and IscX proteins. IscR (a [2Fe–2S] cluster-containing transcriptional regulator of *E. coli*) adjusts the synthesis of the Isc Fe–S biogenesis pathway to maintain Fe–S homeostasis through a negative feedback loop to repress transcription of the isc operon, encoding IscR and the Isc machinery, through binding of [2Fe–2S]–IscR to two upstream binding sites and allows *E. coli* to respond efficiently to varying Fe–S demands. [36] Iron-sulfur cluster assembly initiates when IscS, a cysteine desulfurase that contains the pyridoxal-5'-phosphate (PLP) cofactor, catalyzes the removal of elemental sulfur from free L-cysteine, found in the cell, producing alanine and an enzyme-bound sulfanylcysteine species, often referred to as a persulfide (S^0), that is assembled on an active-site cysteine of IscS. This reaction proceeds to a transpersulfuration step during which the persulfide is transferred to acceptor protein IscU. In the course of the cluster assembly, IscS and IscU form a covalent complex, where the sulfur atom derived from L-cysteine is transferred from IscS to the scaffold protein IscU for the assembly of either [2Fe-2S] or [4Fe-4S] with iron obtained from a currently unknown source.[37,38] These Fe-S clusters can be transferred to acceptor proteins such as IscA, a member of the A-type carrier protein family responsible for Fe-S cluster shuttling.[32,39] HscA and HscB form a chaperone/cochaperone system are believed to facilitate the assembly of clusters on IscU and the transfer of [2Fe-2S] iron-sulfur clusters from the Fe-S-scaffold protein IscU to acceptor proteins in an ATP-dependent manner.[40-42] Ferredoxin (*fdx*) is an iron-sulfur protein that transfers electrons in a wide variety of metabolic reactions and is involved in the *in vivo* assembly of the Fe-S

clusters in a wide variety of iron-sulfur proteins. Although the function of this ferredoxin in the Isc pathway is unclear, it is probable that it has a role as a cellular electron transfer protein. However, ferredoxin can accept [2Fe-2S] clusters from scaffold proteins and A-type carrier proteins.[43] IscX (also referred to as ORF3 or YfhJ) is a small acidic protein is structurally capable of binding to iron. [44] Furthermore, *in vitro* studies have shown that IscX acts as a regulator of iron-sulfur cluster assembly by forming different complexes with IscU and/or IscS.[45-47]

The Suf Pathway

Under oxidative stress and iron starvation conditions,[21,31,48] the Suf pathway is primarily utilized, expressing the following genes of the suf operon: *sufA, sufB, sufC, sufD, sufS,* and *sufE*. For Fe-S cluster biogenesis under the Suf pathway, the PLP-bound SufS protein functions as the cysteine desulfurase, also acquiring sulfur from available pools of cysteine to form the transportable persulfide intermediate.[49,50] SufS requires a shuttle protein (SufE) to participate as a co-substrate in the transpersulfuration reaction, where SufE operates to remove the persulfide and transfers it to the scaffold protein where *de novo* Fe-S cluster biogenesis occurs.[51] The shuttling protein SufE also enhances the low basal activity of SufS by allosterically altering active site residues around the PLP cofactor prior to or concurrent with desulfuration. SufB is the scaffold protein of the Suf system that can transiently assemble a Fe-S cluster during biogenesis. As a scaffold, SufB can interact with the SufE protein that mobilizes persulfide from the cysteine desulfurase SufS active site. The interaction between SufB and SufE is enhanced if SufC, an ABC ATPase, is bound to SufB as $SufB_2C_2$ or $SufBC_2D$ scaffold complexes, on which the nascent Fe-S cluster is assembled.[48,52] $SufBC_2D$ acts as a stress-resistant scaffold complex in *E. coli*,

producing [2Fe–2S] clusters that more stable and resistant to oxidative stress (H_2O_2, O_2) and iron limitation (such as from iron chelators), compared to [2Fe-2S] clusters constructed with IscU (scaffold protein of the Isc pathway).[53] SufB and SufD share a similar structural organization, with an N-terminal helical domain, a core domain consisting of a right-handed parallel β-helix, and a C-terminal helical domain that contains the SufC binding site.[54,55] Structural analysis show that the ATPase activity of SufC likely drives conformational change of its SufB-SufD binding partners resulting in ATP-dependent conformational changes that suitably rearranges the scaffold complex to facilitate Fe-S cluster biogenesis.[55,56] Deletion of *sufD* reduces the iron content of the subcomplex $SufB_2C_2$ and for this reason SufD is thought to play a role in iron acquisition, but the exact function of SufD remains undetermined.[56] The *in vivo* iron donor for the Suf pathway is unknown, but ferric iron is thought to be supplied by an iron storage or iron chaperone protein during Fe-S cluster biogenesis. The Suf pathway also contains an A-type carrier protein (SufA) that can act as an acceptor protein, and studies show that $SufBC_2D$ can transfer its Fe-S cluster to SufA.[43,57] SufA can also assemble Fe-S clusters *in vitro* and transfer those clusters to apo-proteins.[58] In the presence of the $SufBC_2D$ scaffold protein, Fe-S cluster formation onto SufA is enhanced.

A-Type Carrier (ATC) Proteins in E. Coli

A-type carrier (ATCs) proteins are a class of Fe-S cluster trafficking proteins that have important cellular functions in Fe-S cluster metabolism and can be divided into three families: type-I, type-II, and type-III.[32] Phylogenomic studies indicate that there are three A-type carrier proteins in *E. coli* that have evolved into two subfamilies. ErpA, an essential respiratory protein, is classified as a type-I ATC protein. IscA and SufA (encoded by the

isc and *suf* operons, respectively) are designated to the type-II ATC subfamily.[32] Type-III ATC proteins, which are not present in *E. coli*., are a smaller subfamily found within the operon of Fe-S cluster biogenesis genes in nitrogen fixing bacteria and include ^{Nif}IscA.[32] The first subfamily (ATC-I) is thought to transfer Fe-S clusters to target apo-proteins, while the second (ATC-II) receives its clusters from a Fe-S scaffold protein and may act as intermediate carriers between the scaffold and ATC-I carriers.[32] While the exact function of ATC proteins has been subject to debate, it is possible that ATC proteins have multiple distinct biochemical functions such as Fe-S cluster trafficking and iron donation for biogenesis or repair of Fe-S clusters.

Biochemical analyses have clearly demonstrated that ErpA, IscA, SufA, and ^{Nif}IscA homodimers can coordinate either a [2Fe-2S] or a [4Fe-4S] cluster and suggests that these enzymes can deliver the bound Fe-S clusters to apo-proteins *in vitro*.[43,57,59-62] ^{Nif}IscA from *Azotobacter vinelandii* has been shown to bind a [2Fe-2S] cluster in the presence of oxygen, with reversible conversion to a [4Fe-4S] cluster occurring under anaerobic and reducing conditions.[34] Both IscA and ^{Nif}IscA homodimers can efficiently bind a single Fe^{2+} or Fe^{3+} in a mononuclear site, which is coordinated by conserved Cys residues, and results suggest that this process is crucial for Fe-S cluster biogenesis.[34,63] In *E. coli* IscA, a Tyr residue has also been implicated in iron binding, possibly *via* an oxygen ligand.[63] For IscA, the ferric iron can be released in the presence of L-cysteine, presumably by reduction of Fe^{3+} to Fe^{2+}, allowing the iron to be incorporated into nascent cluster assembly on the IscU scaffold *in vitro*.[64] There is some dispute regarding whether *E. coli* SufA also coordinates ferrous and ferric iron in the same manner as IscA, but it seems distinctly possible. Iron-binding properties of ErpA have not been thoroughly investigated.

In vitro and *in vivo* evidence suggests that SufA and IscA interface with their respective scaffolds ($SufBC_2D$ and IscU) and have partially overlapping functions. An Δ*iscA* Δ*sufA* double mutant in *E. coli* grows very poorly under aerobic conditions, showing defects in the maturation of multiple [4Fe-4S] enzymes, indicating that *E. coli* ATC proteins have a specific role in delivering [4Fe-4S] clusters.[32,65,66] Similarly, the ATC I and II homologues *S. cerevisiae* Isa1p and Isa2p have also been clearly linked to maturation of mitochondrial [4Fe-4S] clusters *in vivo*.[67] However, the *E. coli* double mutant strain showed essentially no defective [2Fe-2S] proteins tested in the growth experiment. In contrast, the single deletion strains Δ*iscA* and Δ*sufA* showed relatively mild phenotypes.[59] Multicopy suppressor analysis of strains with combinations of ATC deletions in *E. coli* suggests there is some redundancy between IscA and SufA in their roles as Fe-S cluster trafficking proteins. *In vivo* results also indicate that SufA may provide additional functionality under oxidative stress. All three ATC proteins show similar Fe-S cluster stability when exposed to oxygen *in vitro*.[61] Therefore, it is not clear if SufA itself is more resistant to oxidative stress than IscA, or if it is simply a better transfer partner for the SufS-SufE-$SufBC_2D$ cluster assembly complexes, which have been shown to be more stress resistant than the Isc pathway *in vitro*.

Structure of ATC Protein SufA

The crystal structure of ~13 kDa ATC protein apo-SufA reported by Wada et al. (PDB 2D2A) shows a homodimeric structure in which the two monomers (α_1 and α_2) are stabilized by H-bonding and extensive hydrophobic interactions.[68] The two monomers are oriented such that the C-terminal region of the α_1 monomer interacts with the C-terminus of the α_2 monomer. Similar to other ATC proteins, SufA possesses three highly conserved

cysteine residues that are arranged in a $C_{50}xC_{114}xC_{116}$ motif near the C-terminus of the monomer. The arrangement of these cysteines in proximity to one another ensures efficient binding of iron, [2Fe-2S], and/or [4Fe-4S], as suggested by modeling and biochemical studies.[39,58,60,68] However, the coordination chemistry has not been elucidated at the structural level.. Previous work with homologous ATC proteins *S. cerevisiae* Isa1p and Isa2p, found in the eukaryotic mitochondrion, has demonstrated that each of three conserved cysteine residues is essential for ATC protein activity. [67]

Glutaredoxins in E. coli

Glutaredoxins (Grxs) are members of a highly conserved superfamily of proteins, originally identified as redox proteins involved in thiol-disulfide exchange.[69] Glutaredoxins catalyze the reduction of disulfides via reduced glutathione (GSH), in a coupled system with glutathione reductase (GR) and NADPH.[70] Biochemical characterization studies of both eukaryotic and prokaryotic Grxs have shown that they function in iron homeostasis as Fe donors, in signal transduction (in mammalian systems), and in Fe-S cluster assembly as cluster scaffold or delivery proteins.[71] Grxs may be classified into two categories based on their active site sequence: dithiol Grxs have a CXXC motif (usually CPYC), while monothiol Grxs typically have active-site cysteine-glycine-phenylalanine-serine amino acid sequences (CGFS motif).[70] Although both groups share a similar structure, the CGFS-type Grxs do not function as GSH-disulfide oxidoreductases. Additionally, glutaredoxins can be further divided into subclasses: those with a single Grx domain and the multi-domain proteins comprising an N-terminal thioredoxin-like domain as well as up to three Grx domains. All bacterial monothiol CGFS Grxs are of the single Grx domain type.[62] Four glutaredoxins (Grx1, Grx2, Grx3, and Grx4)

have been described in *E. coli*, of which Grx4 is the only monothiol glutaredoxin and has been associated with Fe-S cluster metabolism.[72] Monothiol Grxs were initially investigated in the yeast *S. cerevisiae*, which possesses three CGFS-type Grxs: Grx3, Grx4, and Grx5 and have a protective role against oxidative stress.[73] *S. cerevisiae* Grx5 is a mitochondrial protein that plays a role in the Fe-S cluster biosynthesis machinery.[74,75] *E. coli* Grx4 was originally characterized as a highly abundant protein with significant sequence identity to *S. cerevisiae* Grx5 and was found to not function as an oxidoreductase, even though it was redox-active and capable of being glutathionylated, or the formation of mixed disulfide bonds with glutathione (GSH).[70] Biochemical studies of a variety of CGFS-type Grxs indicate that a conserved mechanism exists for proteins to adopt either a dimeric conformation bound to a [2Fe-2S] cluster, or to switch to a monomeric apo-form that releases its [Fe2-S2] cluster, which suggests a conserved role for these proteins in both prokaryotes and eukaryotes.[71] The monothiol glutaredoxin family has been shown to store, transport, and transfer a [2Fe-2S] cluster to target proteins, thus acting as delivery proteins of Fe-S clusters. In fact, *in vitro* experiments show that *E. coli* homodimeric Grx4 has the ability to act as a scaffold protein for intact Fe-S cluster transfer to the model [2Fe-2S] acceptor protein *E. coli* apo-ferredoxin.[76] In *E. coli*, Grx4 is a highly abundant soluble protein, and levels of Grx4 were highly elevated upon conditions of iron depletion in the cell, suggesting an iron-related function for the protein.[70] Genome-wide screens for *E. coli* genetic interactions reported the synthetic lethality (combination of mutations leading to cell death, whereas mutation of only one of these genes does not) of a *grxD* mutation when combined with strains defective in Fe-S cluster biosynthesis (*isc* operon) functions.[77] Indeed, *E. coli* Grx4 was shown to help repair the Fe−S cluster on MiaB, a radical SAM

enzyme involved in methylthiolation of certain tRNAs, which appears to utilize a sacrificial [4Fe-4S] cluster.[78] Grx4 forms a [2Fe-2S]-bridged heterodimer with *E. coli* BolA, much like Grx−BolA complexes from other organisms that have been characterized; however, the specific function of this complex is unclear.[76]

Biomedical Significance

The-Suf pathway is well-conserved among both gram-positive and gram-negative bacterial pathogens, including *Mycobacterium tuberculosis* and *Enterococcus faecalis,* where it is essential for viability, acting as the sole source for Fe-S clusters.[79,80] In response to infection, host macrophages (a type of white blood cell of the immune system) use defense mechanisms such as the induction of reactive oxygen species (ROS), nitric oxide, and iron starvation conditions to attack bacterial Fe-S cluster metabolism during phagocytosis, leading to microbe death.[81] The resurgence of antibiotic-resistant bacteria, many of which rely on the *suf* operon, has made the Suf system an attractive target for the design of novel antibacterial compounds.[80] One strategy for antibiotic development is to identify and disrupt important protein-protein interactions (PPIs) from essential pathways. Rationally designed drugs that target PPIs, such as those in Fe-S cluster biogenesis, often have a lesser probability of generating resistance than traditional antibiotics.[80] Additionally, defining the molecular details of dynamic protein–protein interactions is a critical barrier to understanding the Suf pathway for Fe-S cluster biogenesis.

CHAPTER 2

GRX4 TRANSFERS A [2FE-2S] CLUSTER TO SUFA IN *E. COLI*

ABSTRACT

Glutaredoxins are generally known as redox proteins. Biochemical studies show that monothiol glutaredoxins including *Escherichia coli* (*E. coli*) Grx4 can bind and transfer its cluster to apo-proteins such as ferredoxin. The novel role of glutaredoxins in Fe-S cluster metabolism is unclear. However, understanding the role and its interactions may provide a novel therapeutic target for drug treatment. Herein, we biochemically characterize *E. coli* Grx4 using circular dichroism spectroscopies and gel filtration analysis. It is shown that *E. coli* Grx4 coordinates a [2Fe-2S] cluster that can be transferred to *E. coli* A-type carrier protein SufA *in vitro*, which suggests that Grx4 may transfer its cluster to SufA *in vivo*. These results suggest that [2Fe-2S] Grx4 may act as an Fe-S scaffold or delivery protein.

INTRODUCTION

A major biological question in Fe-S cluster trafficking concerns mechanisms of cluster targeting to apo-proteins, which certainly involves recognition by PPIs. As previously described, SufA from *E. coli* is a type II A-type Fe-S cluster carrier (ATC) protein and has been shown to act as the initial acceptor of Fe-S clusters from $SufBC_2D$.[32] While SufA can supply Fe-S clusters to several Fe-S apo-proteins *in vitro*, recent genetic studies suggest that *in vivo* trafficking utilizes a more complex mechanism. A complexity for *in vivo* trafficking is the potential for "cross talk" between pathways under various environmental conditions. Recent genetic studies suggest the monothiol glutaredoxin, Grx4, may act as an intermediary for cluster transfer between the IscU scaffold and SufA, consistent with a cross talk mechanism.[62,74,82-85] Previous genetic evidence suggests that SufA can accept Fe-S clusters from other pathways through a cross talk mechanism. In *E. coli*, one protein that may play a role in iron metabolism is the monothiol glutaredoxin, Grx4.[71,76,78,86] Monothiol glutaredoxin (Grx) proteins can bind [2Fe-2S], linear [3Fe−4S], and [4Fe−4S] clusters as homodimers that include obligate glutathione (GSH) molecules as cluster ligands along with Cys residues.[71,78,87-89] *In vitro* Grx4 can accept a cluster from [2Fe−2S] IscU and transfer clusters to apo-proteins such as Fdx, IscA, and aconitase.[62,76,89,90] However, genetic data casts doubt on a biological role of Grx4 solely in the Isc pathway. Deletion of *grxD* (encoding Grx4) is synthetically lethal under aerobic conditions when combined with *isc* mutations, suggesting they function in separate pathways.[76,77,91] In fact, the Δ*grxD* single mutant strain has growth defects under iron starvation and stationary phase stress conditions similar to defects reported for deletions in the Suf pathway.[76] In support of a Suf connection, *in vitro* Fe-S cluster transfer experiments

on the plant homologues of Grx4 and SufA demonstrated that clusters could be transferred from the plant Grx to the SufA homologue (*A. thaliana* GrxS14 to *A. thaliana* SufA1), where cluster transfer is unidirectional.[62] However, this interaction has not been tested in *E. coli.* Our goal in this work is to test if *E. coli* monothiol glutaredoxin Grx4 can also transfer its cluster to *E. coli* A-type carrier protein SufA, thereby providing a novel Fe-S cluster trafficking pathway in *E. coli.*

MATERIALS AND METHODS

Protein expression and purification

The pET21a vector (Novagen) containing the *E. coli sufA* gene was induced via an inducible isopropyl-β-D-thiogalactoside (IPTG) promoter in order to perform the overexpression of SufA in *E. coli* BL21(DE3) strain cells. Cells were grown in Lennox Broth (LB) media at 37 °C to an optical density (OD) measured at 600 nm of 0.6 to 0.8 before induction with 1mM IPTG at 18 °C and incubated overnight. Cells were collected 18 hours after induction via centrifugation and stored at -80 °C. Cell pellets were resuspended in 25 mM Tris-HCl, pH 7.8, 10 mM (β-mercaptoethanol) βME, and 1 mM phenylmethanesulfonyl fluoride (PMSF) then lysed via sonication. Cellular debris was mixed with 1% streptomycin sulfate and centrifuged at 16,000 rpm at 4 °C to remove cell debris. The cleared cell lysate was loaded onto a DEAE ion exchange column pre-equilibrated with 25 mM Tris-HCl, pH 7.8, and 10 mM βME. SufA eluted between 0.26 M to 0.42 M sodium chloride (NaCl) using a linear gradient starting with Buffer A (25 mM Tris-HCl, pH 7.8, 10 mM βME and 0 M NaCl) to Buffer B (25 mM Tris-HCl, pH 7.8, 10 mM βME, and 1 M NaCl). Fractions containing SufA, as judged by Sodium Dodecyl Sulfate Polyacrylamide Gel Electrophoresis (SDS-PAGE) and UV-visible spectroscopy,

were collected, and loaded onto a Phenyl FF column pre-equilibrated with 25 mM Tris-HCl, pH 7.8, 10 mM βME, and 1 M NH_4SO_4 (ammonium sulfate). SufA eluted at 0.42 M to 0 M NH_4SO_4 using a linear gradient starting from 1 M NH_4SO_4 to 0 M NH_4SO_4. Eluted protein was concentrated using Millipore centrifugal devices and loaded onto the HiLoad Superdex 75 gel filtration column (GE Healthcare) equilibrated with 25 mM Tris-HCl, pH 7.8, 150 mM NaCl, and 10 mM βME. The pure protein was concentrated, flash-frozen in liquid nitrogen, and stored at -80°C.

The pRSFDuet-1 vector (Novagen) containing the *E. coli grx4 (grxD)* gene was induced via an IPTG promoter in order to perform the overexpression of Grx4 in *E. coli* BL21(DE3) strain cells. Cells were grown in LB media at 37 °C to an OD_{600} of 0.6 to 0.8 before induction with 500 μM IPTG at 18 °C and incubated overnight. Cells were collected 18 hours after induction via centrifugation and stored at -80 °C. Cell pellets were resuspended in 25 mM Tris-HCl, pH 7.8, 10 mM βME, and 1 mM PMSF then lysed via sonication. Cellular debris was mixed with 1% streptomycin sulfate and centrifuged at 16,000 rpm at 4 °C to remove cell debris. The cleared cell lysate was loaded onto a DEAE ionic exchange column pre-equilibrated with 25 mM Tris-HCl, pH 7.8, and 10 mM βME. *E. coli* Grx4 eluted between 0.20 M to 0.53 M NaCl using a linear gradient starting with Buffer A (25 mM Tris-HCl, pH 7.8, 10 mM βME, and 0 M NaCl) to Buffer B (25 mM Tris-HCl, pH 7.8, 10 mM βME, and 1 M NaCl). Fractions containing Grx4, as judged by SDS-PAGE and UV-visible spectroscopy, were collected, and loaded onto a Phenyl FF column pre-equilibrated with 25 mM Tris-HCl, pH 7.8, 10 mM βME, and 1 M NH_4SO_4. Grx4 eluted at 0.25 M to 0 M NH_4SO_4 using a linear gradient starting from 1 M NH_4SO_4 to 0 M NH_4SO_4. Eluted protein was concentrated using Millipore centrifugal devices and

loaded onto the HiLoad Superdex 75 gel filtration column (GE Healthcare) equilibrated with 25mM Tris-HCl, pH 7.8, 150mM NaCl, and 10 mM βME. The pure protein was concentrated, flash-frozen in liquid nitrogen, and stored at -80 °C.

Protein Expression and Purification of his tagged GRx4

The pBAD/*Myc*-His C vector (Invitrogen) containing the gene for recombinant His_6-Grx4 protein was induced via a L-arabinose promoter in order to perform the overexpression of His_6-Grx4 in *E. coli* Top10 strain cells. Cells were grown in LB media at 37 °C to an OD_{600} of 0.6 to 0.8 before induction with 0.05% L-arabinose at 18 °C. Cells were collected 6 hours after induction via centrifugation and stored at -80 °C. Cell pellets were resuspended in lysis buffer containing buffer A (50 mM Tris-HCl, pH 7.4, 500 mM NaCl, 20mM imidazole, and 10 mM βME), 1 mM PMSF, 10 μg/ml DNase I, and 2 mM $MgCl_2$, then lysed via sonication. Cellular debris was centrifuged at 16,000 rpm at 4 °C to remove cell debris. The cleared cell lysate was loaded onto a HisTrap HP column pre-equilibrated with Buffer A. *E. coli* Grx4 eluted between 0.15 M to 0.21 M imidazole using a linear gradient starting with Buffer A to Buffer B (50 mM Tris-HCl, pH 7.4, 500 mM NaCl, 500 mM imidazole, and 10 mM βME). Fractions containing His_6-Grx4, as judged by SDS-PAGE and UV-visible spectroscopy, were concentrated and desalted using Millipore centrifugal devices. The pure protein was flash-frozen in liquid nitrogen and stored at -80 °C.

In vitro Fe-S Cluster Reconstitution of Proteins

The preparation of apo-proteins, or proteins without an Fe-S cluster, was conducted by treating purified protein (1 mM) with a 50-fold molar ratio of ethylenediaminetetraacetic acid (EDTA) and 20-fold molar ratio of ferricyanide for 10 to

60 minutes on ice or until loss of color from any Fe-S cluster occurred, followed by desalting.[92] In order to form a holoprotein, or a protein that contains an Fe-S cluster, reconstitution of an Fe-S cluster on apo-Grx4 (1 mM in 25 mM Tris-HCl, pH 7.8, and 150 mM NaCl) was carried under anaerobic conditions (O_2 < 5 ppm) in a glove box (Coy Laboratory Products, Grass Lake, MI). The reaction mixture involved 2 mM glutathione (GSH), 5 mM dithiothreitol (DTT), a 8-fold molar excess of ferrous ammonium sulfate (FAS) and a 10-fold molar excess of L-cysteine, and catalytic amounts of *E. coli* SufS and SufE (4 μM). The reconstitution mixture was incubated under strictly anaerobic conditions for 1 hour on ice with occasional stirring. Cluster formation was monitored by UV-Visible absorption spectroscopy and Circular Dichroism (CD) spectroscopy. Reagents in excess were removed anaerobically by loading onto a Q-Sepharose FF column (GE Healthcare) pre-equilibrated with buffer (25 mM Tris-HCl, pH 7.8), inside the glove box. pre-equilibrated with reconstitution buffer. Elution was achieved using a NaCl gradient with cluster-bound Grx4 eluting between 0.60 and 0.70 M NaCl. Samples were pooled together as a single fraction before concentrating and desalting using Millipore centrifugal devices. The same protocol was followed for reconstitution of an Fe-S cluster on apo-SufA, except that GSH was excluded from the reaction mixture.

Biochemical Analyses

Protein concentrations were determined by the Bradford assay (Bio-Rad) using bovine serum albumin (BSA) as the standard. Iron concentrations were determined using the colorimetric ferrozine assay as previously described.[93] Acid-labile sulfur concentrations were determined using published methods.[94,95]

Analytical and spectroscopic methods

Analytical gel filtration analyses were performed on a Superdex 75 10/300 GL column (GE Healthcare) connected to an AktaGo FPLC system (Cytiva) and a 100 μL sample loop at a flowrate of 0.5 mL / min. For protein oligomeric state determination on as-purified protein, the column was equilibrated with room temperature aerobic reducing buffer (50 mM Tris–HCl, pH 8.0, 500 mM NaCl, 5 mM TCEP). Calibration was performed with the Low Molecular Weight Gel Filtration Calibration kit (GE Healthcare) in room air. For protein interaction studies, the column was equilibrated with room temperature gel filtration buffer (50 mM Tris–HCl, pH 7.8, 500 mM NaCl, 1 mM GSH) unless other with specified. Calibration was performed with the Low Molecular Weight Gel Filtration Calibration kit (GE Healthcare) as previously described.[87] Briefly, the buffer was bubbled with N_2 overnight and degassed to minimize dissolved O_2 levels. Air sensitive samples (i.e., reconstituted Fe-S cluster containing proteins) were taken out of the anaerobic chamber in gas tight syringes and loaded immediately onto the column. Elution profiles were recorded at 280 nm with a flow rate of 0.5 mL/min. The same set of fractions was collected for all proteins eluted from gel filtration and were analyzed by SDS-PAGE in order to compare relative elution times. UV-visible absorption spectra were recorded using a Beckman DU-800 and CD spectra were recorded on identical samples using a Jasco J-810 spectropolarimeter (Jasco, Hachioji, Japan) using a 1cm cuvette.

Ni-NTA affinity chromatography assay to characterize protein-protein interactions between His_6-Grx4 with apo-SufA

All steps were carried out anaerobically in a Coy chamber. In the first method, equimolar amounts of holo His_6-Grx4 and apo-SufA were combined in an Eppendorf tube

and allowed to incubate for 5 min. before loading onto the column. The column then was washed with 3 mL of binding buffer (50mM tris-HCl, pH 7.4, 0.5 M NaCl, and 20 mM imidazole). Then His_6-Grx4 and any proteins bound to it were eluted with elution buffer (50mM tris-HCl, pH 7.4, 0.5 M NaCl, and 500 mM imidazole). All wash and elution fractions were collected and concentrated separately using Nanosep centrifugal devices. Equal volumes of elution fractions (concentrated to the same final volume) were separated by SDS-PAGE. As a control, apo-SufA was loaded, washed, and eluted on a Ni-NTA column containing no His_6-Grx4 protein to determine whether non-specific SufA binding to the Ni-NTA column is observed. The interaction between apo-His_6-Grx4 and apo-SufA was also tested by incubating equimolar amounts in an Eppendorf tube and allowed to incubate for 5 min. before loading onto the column, followed by a subsequent column washing step.

In the second method, The Ni-NTA 1-mL column was charged with 50 nmol of freshly prepared holo His_6-Grx4 protein (reconstituted and purified as described above). Next 30 nmol apo-SufA was loaded on the column and allowed to incubate for 5 min prior to resuming flow. The column then was washed with 3 mL of binding buffer. Then His_6-Grx4 and any proteins bound to it were eluted with elution buffer. All wash and elution fractions were collected and concentrated separately using Nanosep centrifugal devices. Equal volumes of elution fractions (concentrated to the same final volume) were separated by SDS-PAGE. As a control, apo-SufA was loaded, washed, and eluted on a Ni-NTA column containing no His_6-Grx4 protein to determine whether non-specific SufA binding to the Ni-NTA column is observed.

Fe-S Cluster Transfer Monitored by Circular Dichroism Spectroscopy

Apo-Grx4 was reconstituted as previously described. CD experiments were performed using a Jasco J-810 spectropolarimeter. Measurements were performed with a 1-cm path length cuvette in reaction buffer (25 mM tris-HCl, 150 mM NaCl, pH 7.8). In order to characterize the interaction between SufA and [2Fe-2S] Grx4, as-purified SufA and reconstituted [2Fe-2S] Grx4 were mixed in reaction buffer at a 2:1 ratio of [SufA]:[2Fe-2S] and scans were taken at 10 min intervals for 1 h at room temperature.

After a 10-min anaerobic incubation, the Fe-S cluster transfer was monitored every 10 minutes with UV-visible and CD spectra taken to compare with that of reconstituted [2Fe-2S] Grx4. As a control, the reconstituted [2Fe-2S] Grx4 alone (80 μM iron content, 40 μM cluster) was scanned at 0- and 1-hour at room temperature in a 1 cm path length anaerobic cuvette to determine Fe-S cluster stability.

CD-monitored titrations of [2Fe-2S] Cluster-Bound Grx4 with apo-SufA

The titration of [2Fe-2S] cluster-bound Grx4 with apo-SufA was monitored under anaerobic conditions at room temperature using UV−visible CD spectroscopy. Reactions were conducted in 50 mM tris-HCl, 150 mM NaCl, pH 7.8, 1 mM GSH (interaction buffer), with the [2Fe-2S] cluster concentration kept constant at 100 μM and SufA: [2Fe-2S] ratios varying from 0 to 6. A series of individual samples were anaerobically prepared, each containing an increasing amount of SufA that was added to [2Fe–2S] Grx4 up to a 6 : 1 ratio of SufA to [2Fe–2S]. Samples were equilibrated for 5 min. at room temperature after addition of SufA prior to recording CD spectra. All samples were prepared and scanned under anaerobic conditions, and SufA was pre-incubated with 5 mM DTT to reduce any disulfides formed during purification, and then desalted anaerobically before mixing with

[2Fe–2S] Grx4. As a control, holo-SufA was incubated with apo-Grx4 to determine whether the transfer reaction is bi-directional.

Reduction, Alkylation, and Trypsin Digestion of SufA

Reduced SufA was prepared by buffer exchange of pooled protein fractions into reducing buffer (100mM ammonium bicarbonate and 6 M urea) followed by addition of 5 mM DTT and incubation at 56 °C for 45 min to reduce disulfide bonds. The sample was alkylated by incubation with 14 mM iodoacetamide at room temperature for 30 min and in the dark to alkylate cysteines. Unreacted iodoacetamide was quenched by addition of 5 mM DTT and incubated 15 min at room temperature in the dark. Trypsin digestion of protein was accomplished by diluting the protein mixture 1:5 in 100mM ammonium bicarbonate, to reduce the concentration of urea to < 2 M, followed by addition of 1 mM calcium chloride ($CaCl_2$). Trypsin was added at a minimum concentration of 4–5 ng /µl and 1/100–1/200 enzyme: substrate and incubated at 37 °C overnight. Trypsin digestion was halted by acidification with trifluoroacetic acid (TFA) to 0.4% (vol/vol) until the solution pH was < 2.0. The sample was centrifuged at 2,500 × *g* for 10 min at room temperature and the pellet discarded. The sample was dried in a Speedvac Plus Sc110a centrifuge concentrator (Savant) at low temperature. The lyophilized protein was resuspended in 2% acetonitrile / 0.5% formic acid to a peptide concentration of 1-10 µg / µl for Electrospray Ionization-Liquid Chromatography- Mass Spectrometry (ESI-LC-MS) analysis.

RESULTS

Characterization of as-purified E. coli Grx4

It has been well-established that monothiol glutaredoxins form homodimers with a bridging [2Fe-2S] cluster via their active site cysteines and two non-covalently bound glutathione molecules.[71,87,88] Aerobic expression and purification of Grx4 yielded a colorless, clear protein concentrate, and thus, was characterized with spectroscopic and biochemical analysis. Iron and acid-labile sulfur analyses of the aerobically purified Grx4 indicated the protein is monomeric, containing less than 0.01 Fe / 0.05 S per monomer. As-purified Grx4 shows no distinct UV-visible or CD spectra peaks due to the absence of a homodimer binding pocket. The theoretical monomeric weight of Grx4, according to the amino acid sequence, is approximately 12.9 kDa (Table 2.1). Analytical gel filtration analyses using protein standards of known molecular weight (MW) and diameter (Figure 2.1) confirmed the as-purified oligomeric state of Grx4 to be monomeric protein (Figure 2.2, red line), with an apparent molecular weight of 14.7 kDa.

Characterization of reconstituted Grx4: Grx4 binds a [2Fe-2S] cluster similar to other monothiol glutaredoxins

Due to the loss of Fe-S content during purification, it was necessary to semi-enzymatically reconstitute Grx4. As-purified *E. coli* Grx4 (1 mM) was reconstituted by incubation in an anaerobic glove box (Coy) in reconstitution buffer containing 25 mM Tris-HCl, pH 7.8, 150 mM NaCl, 5 mM dithiothreitol (DTT), 2 mM glutathione (GSH), with 10-fold excess of L-cysteine and ferrous ammonium sulfate (FAS) and 4 μM SufS and SufE. The UV-visible absorption and CD spectra were monitored over time during the reconstitution of *E. coli* Grx4 (Figure 2.3). The reconstitution reaction of Grx4 showed

Table 2.1. Molecular mass analysis of SufA and Grx4 complexes[a]

Sample	Oligomer	Gel Filtration	Theoretical
Apo-Grx4	Monomer	14.7 ± 0.30	12.878
Apo-SufA	Monomer	17.1 ± 0.93	13.300
[2Fe-2S] Grx4	Dimer	34.1 ± 0.56	25.756
Apo-Grx4-SufA	Dimer	28.8 ± 0.68	26.178
[2Fe-2S] Grx4-SufA	Dimer	27.8 ± 0.37	26.178
Apo-SufA	Dimer	25.5 ± 0.33	26.600

[a] All masses are shown in kDa.

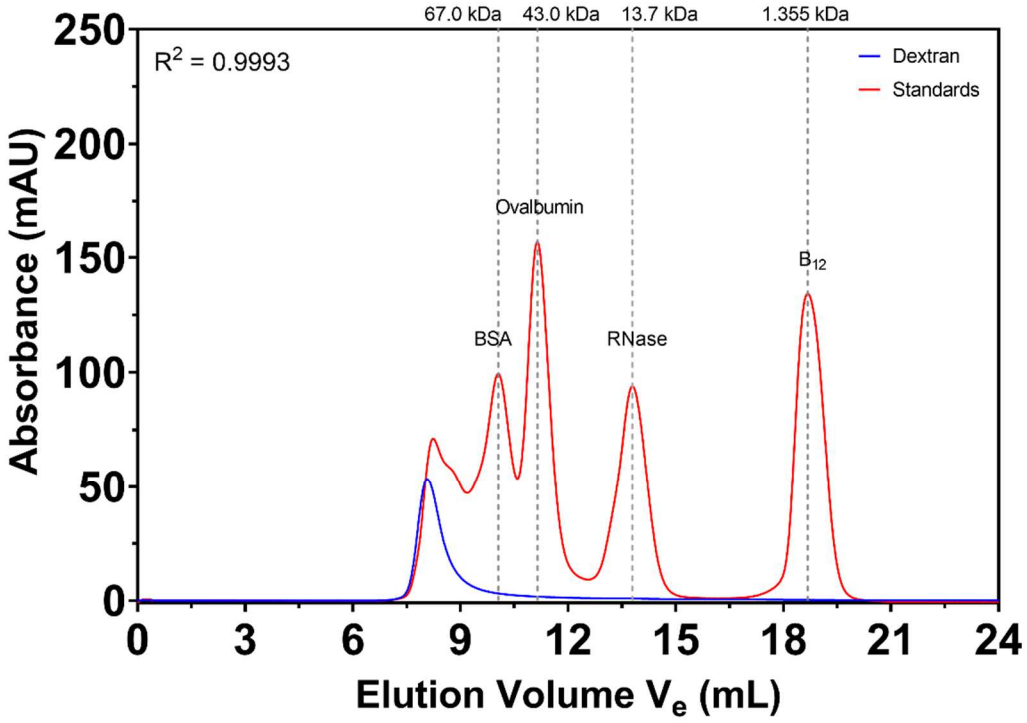

Figure 2.1. Gel filtration chromatograms (1−8 mg loaded) of molecular mass standards (red) and blue dextran (blue). The elution positions of molecular mass standards are shown at the top of the chromatogram.

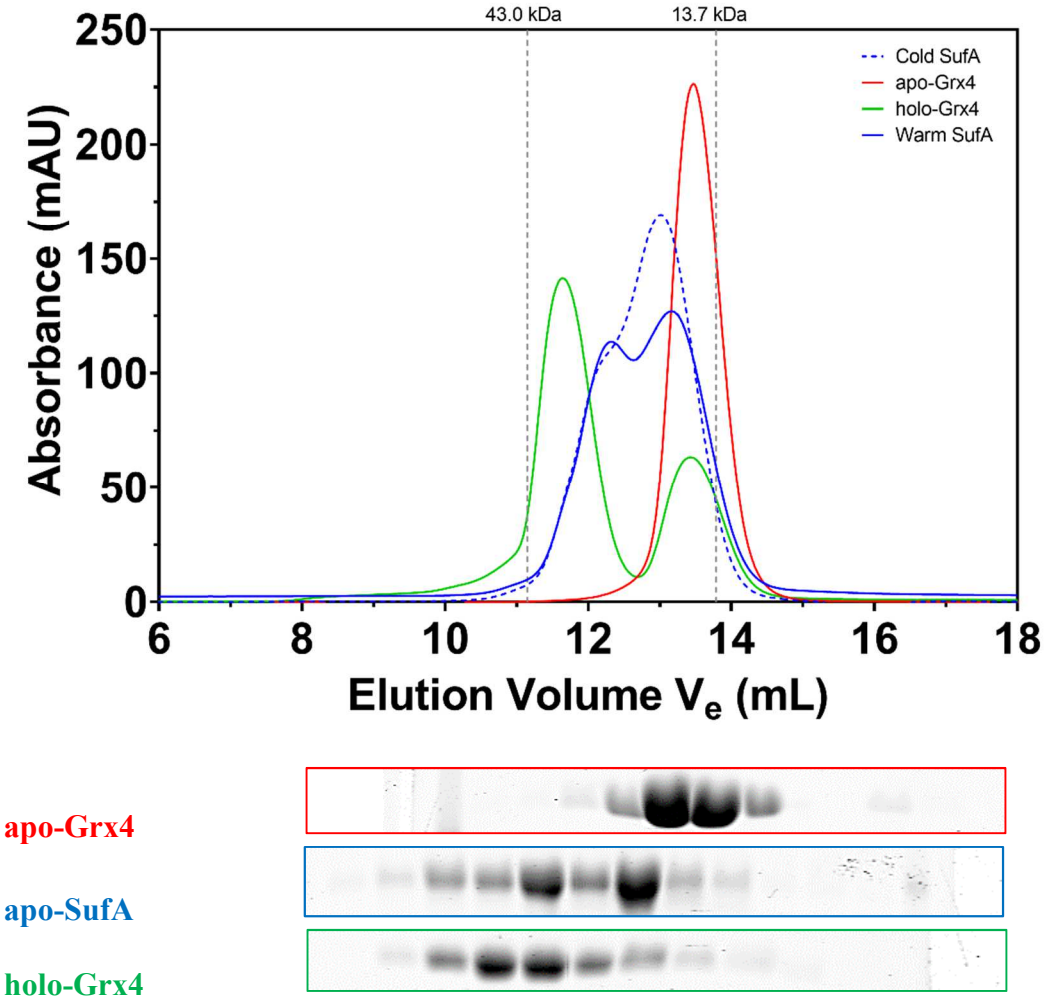

Figure 2.2. Size-exclusion chromatography analysis of Grx4 and SufA Elution Profiles. Top: Gel filtration chromatograms (0.5−1 mg loaded) of apo SufA (blue), apo Grx4 (red), [2Fe-2S] Grx4 (green). The elution positions of molecular mass standards are shown at the top of the chromatogram. Bottom: SDS-PAGE analysis of the fractions collected.

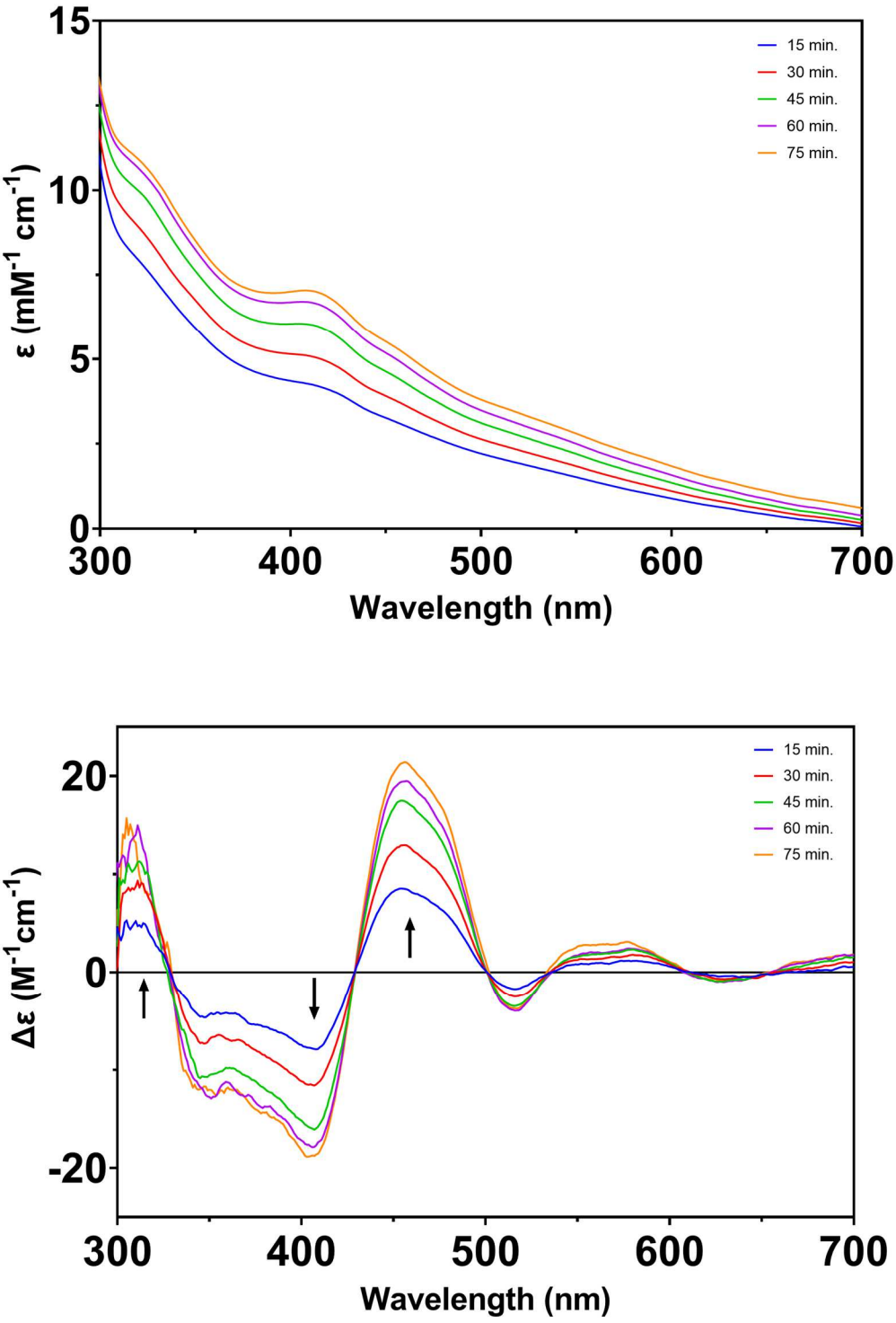

Figure 2.3. Time course of Fe-S cluster formation on *E.coli* Grx4. Monitored by UV-visible absorption (top) and UV-visible CD spectroscopy (bottom) under anaerobic conditions in semi-micro 1 cm cuvettes at room temperature. Δε values are based on the final [2Fe-2S] cluster concentration. The arrows indicate the direction of intensity change with time ats elected wavelengths.

low-level formation of thio-ferrates, or iron-sulfur chain, by-products. This side reaction can be monitored by an increase in absorption at 600 nm. *E. coli* Grx4 reconstitution reached completion after approximately 60 minutes. The reaction was purified by anaerobic anion exchange chromatography using a Hitrap Q FF 1-mL column in order to remove by-products from the reconstituted holo-protein. Iron and acid-labile sulfur analyses of the anaerobically prepared Grx4 complex indicated that the complex contained ~0.75 [2Fe-2S] cluster per homodimer. Reconstitution of *E. coli* Grx4 yielded a [2Fe-2S] bound complex with spectral characteristics identical to what was previously reported in the literature.[76] *E. coli* holo-Grx4 has a distinct UV-visible and CD spectra in the 300 nm to 600 nm range and represents the Fe-S cluster coordination environment of the protein. The UV-visible absorption spectrum of reconstituted Grx4 is nearly identical to other monothiol glutaredoxins from *S. cerevisiae* Grx3 and *Schizosaccharomyces pombe* Grx4, with absorbance peaks at 318, 413, and 455 nm, indicative of a [2Fe-2S] cluster (Figure 2.4A). As expected, the CD spectra for *E. coli* Grx4 was also comparable to *S. cerevisiae* Grx3 and *S. pombe* Grx4. Positive peaks at 308, 455, and 550-590 nm and negative peaks at 345, 404, and 518 nm are characteristic of [2Fe-2S] cluster-bound Grx4 (Figure 2.4C, red line). The stability of *E. coli* holo-Grx4 was observed using CD spectroscopy, where the sample was anaerobically incubated for 1 hour at room temperature, after which its CD signal was measured (data not shown). The CD spectra did not appreciably change, indicating that *E. coli* holo-Grx4 is stable enough at room temperature in order to proceed with further protein-protein interaction studies.

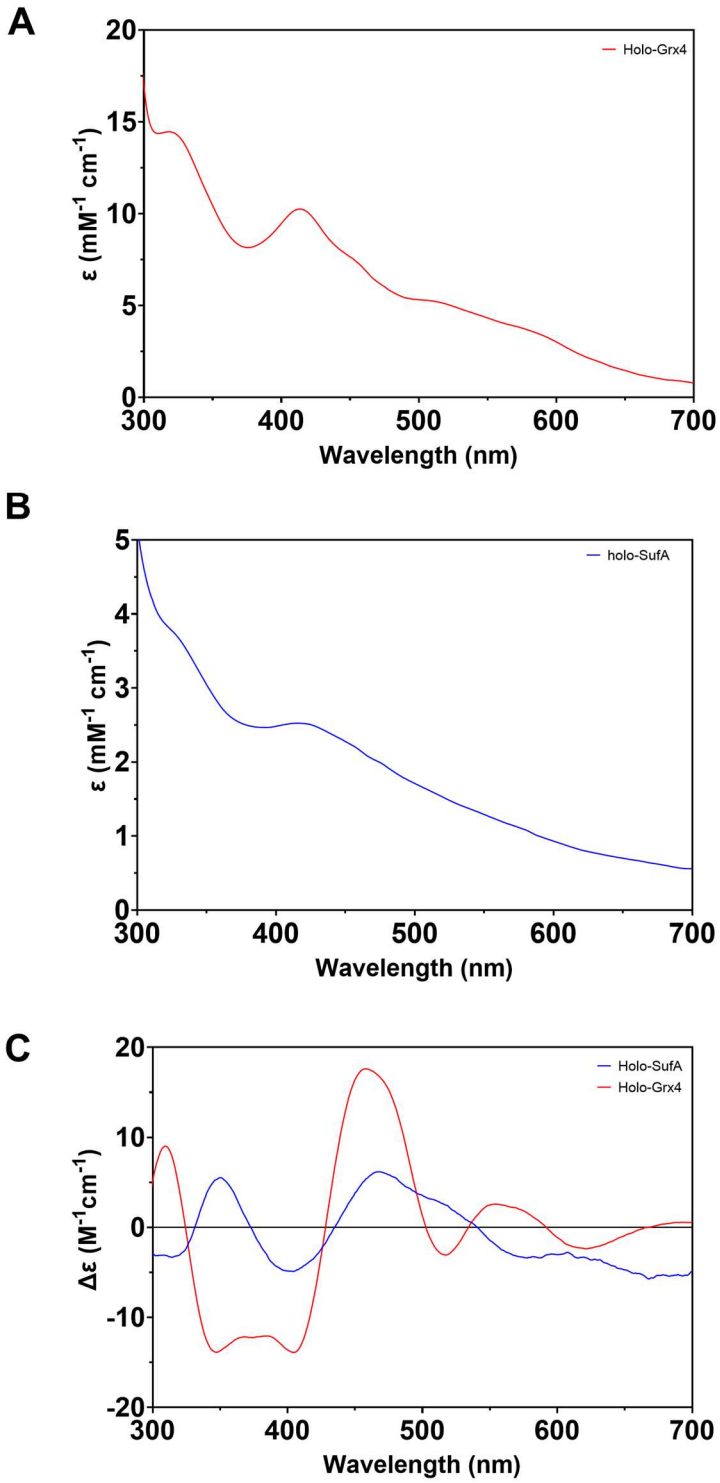

Figure 2.4. Comparison of UV−visible absorption (top) and CD (bottom) spectra of the purified [2Fe-2S] Grx4 homodimer (red) and the [2Fe-2S] SufA homodimer (blue). ε and Δε values are based on the [2Fe-2S] concentration. Spectra were recorded under anaerobic conditions in sealed 0.1 cm cuvettes in 50 mM Tris-HCl buffer with 150 mM NaCl at pH 7.8. Δε values are based on the [2Fe-2S] cluster concentrations.

Oligomeric State of Purified A-Type carrier protein SufA in E. coli

A-type carrier proteins have Fe-S clusters that are semi-stable in air and partially maintained during aerobic purification. The pure SufA protein used in this study always had variable amounts of Fe (0.02 - 0.18 per monomer) in its as-purified form and was converted to its fully apo-form following published procedures.[92] The ATCs have distinct UV-visible and CD spectra in the 300 nm to 600 nm range that represents the Fe-S cluster coordination environment of the individual proteins, as seen for *E. coli* SufA (Figure 2.4). Spectra recorded for SufA after aerobic purification showed weak signal strength in its UV-visible and CD spectra peaks due to the relative absence of a Fe-S cluster in the active site binding pocket (data not shown). The theoretical monomeric weight according to the amino acid sequence of SufA is approximately 13.3 kDa (Table 2.1). Analytical gel filtration analyses using protein standards of known molecular weight and diameter (see Figure 2.1) determined that the as-purified oligomeric state of SufA was likely a monomer-dimer protein mixture (Figure 2.2, blue line), with an apparent molecular weight of 17.1 kDa and 25.5 kDa for the mixture. However, the oligomeric state of SufA was not conclusively determined, as pure SufA protein was expected to elute as a singular protein elution peak. Based on ATC protein homologues, it seems a common property of these proteins to form a mixture of oligomeric states when purified.[58,96-100] Normally, SufA is a dimer in solution, and it shares with IscA the ability to bind [2Fe–2S] and [4Fe–4S] clusters after chemical reconstitution.[39,58]

Characterization of Reconstituted As-Purified E. coli SufA

Due to some loss of Fe-S cluster content during aerobic purification, A-type carrier protein SufA was reconstituted by incubation with ferrous ammonium sulfate (FAS), L-

cysteine, dithiothreitol (DTT), SufS, and SufE under anaerobic conditions. Briefly, the apo-proteins were obtained by incubating the proteins with EDTA and potassium ferricyanide (molar ratios 1:50:20) on ice for 5-10 min followed by desalting. Pre-reduced SufA (1 mM) was incubated in an anaerobic glove box (Coy) in reconstitution buffer containing 25 mM Tris, pH 7.8, 150 mM NaCl, 5 mM DTT, with 10-fold excess of L-cysteine and FAS, and 4 μM SufS and SufE. The iron and acid-labile sulfur analyses of reconstituted SufA showed that the cluster content was 1.38 Fe/monomer, 1.30 S/monomer, indicating that SufA binds a [2Fe-2S] cluster similar to other A-type carrier proteins. The UV-visible absorption spectrum of reconstituted SufA displayed two broad absorption bands at 330 and 420 nm that are characteristic of a [2Fe-2S] cluster on SufA (Figure 2.4B).[39,58,60,101] The CD spectra of holo-SufA alone has well-defined features in the visible region, including positive (+) maxima at 350 and 465 nm, negative (-) maxima at 313, 400, and 575 nm, and complex negative features from 500 – 700 nm (Figure 2.4C, blue line). Therefore, CD spectroscopy can be used to specifically monitor the Fe-S cluster binding of SufA during the cluster transfer reaction without separating the mixture by anaerobic chromatography. The CD spectra of reconstituted and purified holo-SufA is more intense than the as-purified sample, suggesting that the reconstituted proteins contain a much higher quantity of iron in comparison (data not shown). The stability of the protein was observed using CD spectroscopy, where the sample was anaerobically incubated for 1 hour at room temperature, after which its CD signal was measured (data not shown). Reconstituted SufA showed minimal change in its CD spectra, indicating that *E. coli* holo-SufA is stable enough at room temperature in order to proceed with further protein-protein interaction studies.

Gel Filtration Studies Examining the Interactions Between SufA And Grx4

In order to characterize the protein-protein interactions between SufA and Grx4, the individual proteins were initially expressed and purified separately for *in vitro* analysis. Soluble wild-type SufA and Grx4 were easily extracted from *E. coli*, yielding the monomeric apo-forms upon aerobic purification. Analytical size exclusion chromatography (SEC) was performed, which separates protein components in a mixture based on their size and shape. The two proteins were first characterized as apo-proteins (lacking the iron-sulfur cluster) to determine to what degree apo-Grx4 and apo-SufA interact to form a stable complex. These two apo-proteins were predicted to not form a stable complex in the absence of the necessary iron-sulfur cluster since the active form of Grx4 is a homodimer that binds a [2Fe-2S] cluster ligated by two glutathiones, whereas the apo-form of this protein exists in a monomeric form. As previously discussed, the apo-Grx4 was found to purify as a monomeric protein, based on its single elution peak in the SEC chromatogram (Figure 2.2, top, red line), comparably to previously published results, with an apparent molecular weight of 14.7 kDa (Table 2.1), computed using the analytical calibration curve (see Figure 2.1). The Grx4 protein elution fractions were observed on the sodium dodecyl sulphate–polyacrylamide gel electrophoresis (SDS-PAGE) gel, which is a method to separate proteins by molecular mass, as a monomeric protein band corresponding to its theoretical 12.9 kDa size (Figure 2.2, bottom). On the other hand, as previously discussed, the as-purified SufA protein was found to purify as two oligomeric states under the conditions used (see Figure 2.2, blue lines). The elution profile of SufA tended to vary in chromatographic features; for example, when the sample was thawed on ice and loaded onto the column while still cold, the resulting elution profile was a single

chromatographic peak with a shoulder feature, which is evidence of peak splitting, where the signal shape is created by two components eluting close together. One method of testing this hypothesis was to inject a smaller sample concentration onto the column, with the intent to have better separation of any overlapping elution peaks, but the result was an elution peak with the same shape, at a lower absorbance intensity (data not shown). When the frozen SufA protein sample was allowed to warm up to room temperature, the eluting protein separated into two discernable peaks on the chromatogram, seen as a sawtooth pattern. The peaks were calculated to have apparent molecular weights of 17.1 kDa and 25.5 kDa (Table 2.1). The theoretical molecular weight of monomeric SufA is 13.3 kDa and as a dimeric structure is 26.6 kDa, which its published crystallographic structure predicts is the native state of SufA in the *E. coli* cell. Results from running the SEC elution fractions on an SDS-PAGE gel showed a faint protein band with a MW of about 30 kDa (which may be dimeric SufA or a protein contaminant) and a main band at ~14 kDa, which should correspond to monomeric SufA (Figure 2.5). Since the gel contains both the surfactant SDS (sodium dodecyl sulfate) to denature proteins and the reductant β-mercaptoethanol (βME) to cleave disulfide bonds, the SDS-PAGE gel should only contain bands for monomeric proteins. To determine whether the larger MW peak was a possible co-purifying contaminant, the SEC elution fractions corresponding to the higher MW peak were pooled together and proteolytically digested for mass spectral analysis using ESI-LC-MS. The elution peak was identified as 100% *E. coli* SufA, which leads to the hypothesis that the two chromatogram peaks represent a dimer/monomer oligomeric mixture, but the evidence is not conclusive. The fractions corresponding to the higher MW peak (25.5 kDa) were pooled, nondestructively concentrated, and reloaded onto the SEC analytical column

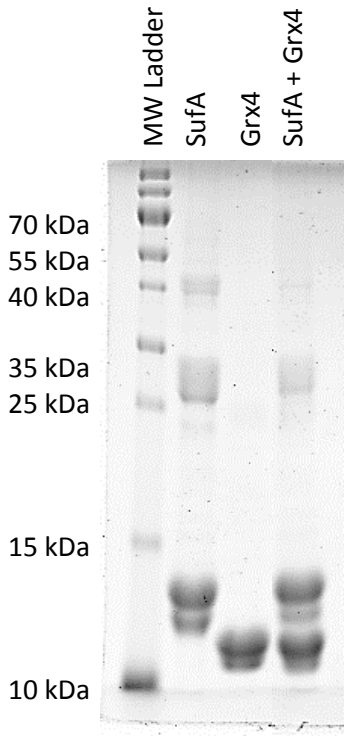

Figure 2.5. SDS-PAGE gel analysis of protein stocks. Purified apo SufA, apo Grx4, and equimolar apo-apo SufA-Grx4 mixture.

using room temperature buffer. The chromatogram showed that this SufA oligomer re-equilibrated, eluting as two peaks corresponding to similar molecular weights as in the original sample result (17.6 kDa and 28.2 kDa) (Figure 2.6, pink line). In contrast, when the lower MW peak fractions were pooled, concentrated, and reloaded onto the column, the resulting chromatogram contained just one peak with a molecular weight (15.8 kDa) similar to the original profile (Figure 2.6, teal line). While the new computed MWs are not identical to the MWs of the original SufA sample, they fall within the margin of error for the resolution of the column used. These results indicate that the larger MW oligomer (dimer) re-equilibrated into a smaller (monomeric) oligomer. This conclusion is supported by evidence from the literature, in which variation in oligomeric states has been reported in the A-type protein family. For instance, *A. vinelandii* ^{Nif}IscA, *Erwinia chrysanthemi* SufA, and *Synechocystis* PCC6803 IscA1 are dimeric proteins.[58,96-98] Experiments suggest that *S. pombe* Isa1 is most likely a tetramer,[99] whereas *E. coli* IscA has been purified as a mixture of dimers and tetramers (a dimer of dimers).[100]

To determine whether apo-Grx4 and apo-SufA interact and to what degree they form a stable complex, equimolar concentrations of each protein were mixed together in a buffer containing 1 mM glutathione (GSH), which is a cofactor needed by Grx4 that aids in coordination of the Fe-S cluster. The resulting chromatogram contained two overlapping elution peaks with a similar profile as compared to SufA pure protein, but with a higher signal intensity (Figure 2.7, top, purple line). The downfield peak had a nearly identical elution volume to monomeric SufA, but the upfield peak eluted with an apparent MW of 28.8 kDa that does not correspond to an oligomer of either pure protein (Table 2.1). The SDS-PAGE gel shows that both elution peaks contain a mixture of SufA and Grx4

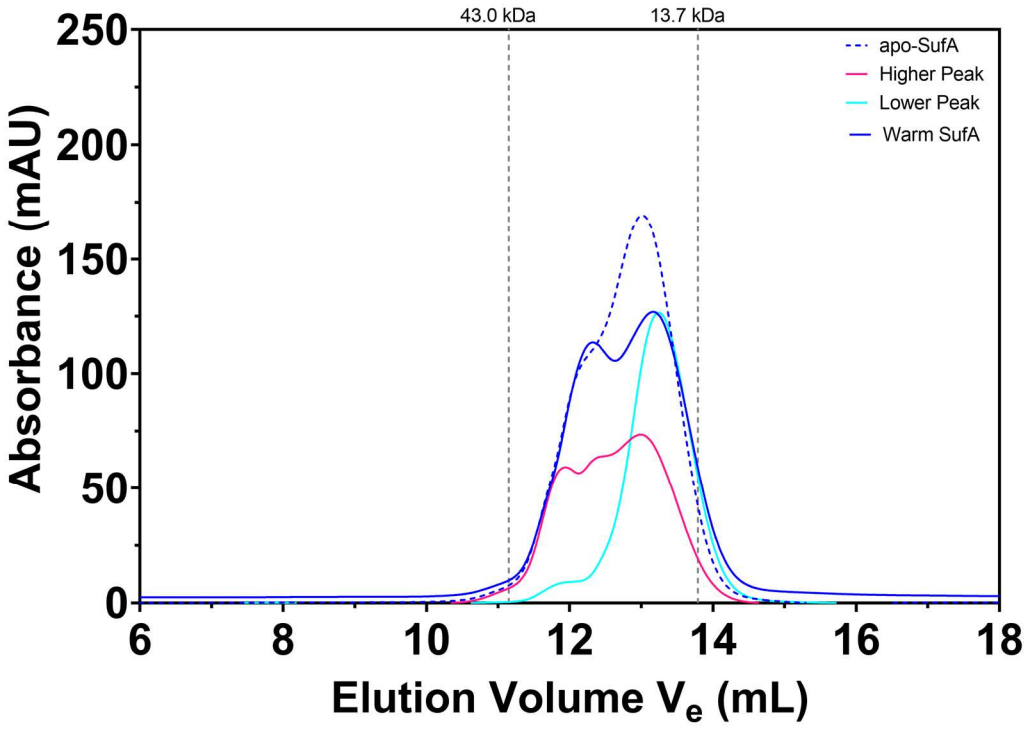

Figure 2.6. Size-exclusion chromatography analysis of SufA Oligomeric States. Gel filtration chromatograms (0.5−1 mg loaded) of apo-SufA (dotted blue), higher molecular weight peak (pink), lower molecular weight peak (teal). The elution positions of molecular mass standards are shown at the top of the chromatogram.

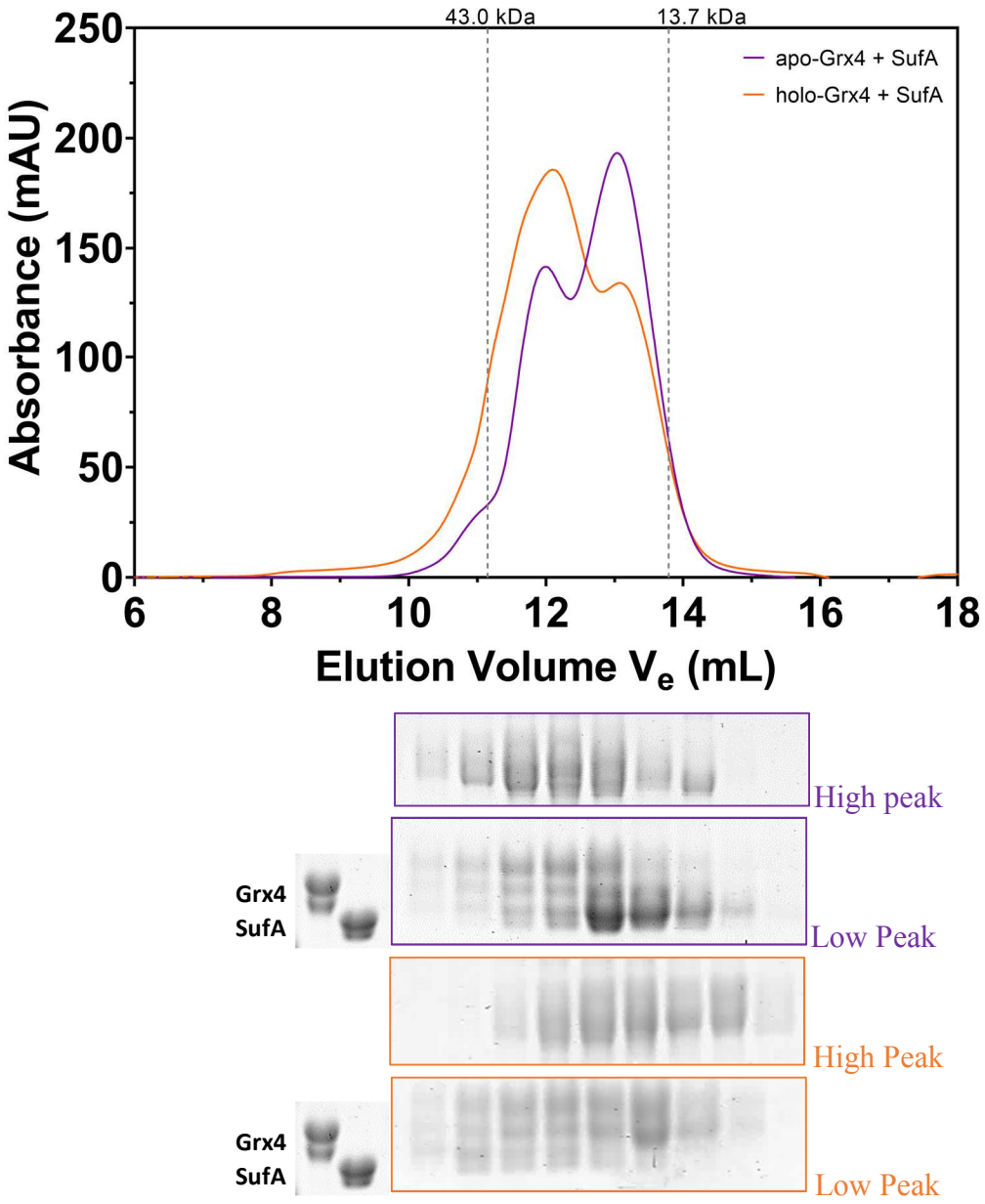

Figure 2.7. Size-exclusion chromatography analysis of Grx4−SufA interactions. *Top*: Gel filtration chromatograms (0.5−1 mg loaded) of apo Grx4 and apo SufA (orange), and [2Fe-2S] Grx4 and apo SufA (purple). SufA and Grx4 were mixed in a 1:1 ratio. The elution positions of molecular mass standards are shown at the top of the chromatogram. *Bottom:* SDS-PAGE analysis of the fractions collected.

(Figure 2.7, bottom), with the upfield peak appearing to produce two main bands corresponding to pure SufA and Grx4 as well as additional bands above the 25 kDa MW standard that does not correlate to either apo-SufA or apo-Grx4. The presence of a heterocomplex cannot be decisively concluded because the individual elution fractions were treated with trichloroacetic acid to quickly concentrate the proteins present in the SEC samples, which may have inadvertently created nonnative heterocomplexes in the samples through the creation of polysulfide bonds.

When the reconstituted (holo) Grx4 sample, which contained ~0.75 [2Fe-2S] cluster per homodimer, was loaded onto the SEC column using anaerobic buffer (Fig. 2.2, green line), the chromatogram result contained two distinct elution peaks. The taller peak corresponded to the Grx4 dimer, with a MW of 34.1 kDa, while the smaller peak represented the Grx4 monomer, with a MW of 15.1 kDa, and this data is corroborated by published results.[102] Monomeric Grx4 was present in small abundance, as expected, because the prepared holo-Grx4 was a dimer/monomer mixture from incomplete Fe-S cluster reconstitution. Nevertheless, some degradation of the homodimer may have occurred as the result of thawing or exposure to air that entered the SEC column through the buffer line. Each fraction of the elution profile was analyzed with CD spectroscopy, which characterizes chirality in molecules through their optical activity, to determine whether distinctive spectral features existed in the samples. The fraction corresponding to the Grx4 homodimer produced the strongest CD signal relative to background noise, whereas the fraction containing the Grx4 monomer peak produced no significant CD signal (data not shown). The CD spectrum for Grx4 homodimer contained a broad negative peak at ~340 - 410 nm and a positive broad peak at ~470 nm, which is comparable to previous

findings (see Figure 2.4C, red line). These results confirm that the reconstituted Grx4 protein was in a dimer conformation, which is the active oligomer that binds the iron-sulfur cluster. Holo-Grx4, when exposed to room air, has a loss of the Fe−S cluster absorbance signal over time in the 300−600 nm region. Apo-Grx4 does not produce a CD signal because as a monomer it has no chirality so there is no absorption of left and right circularly polarized light.

To determine whether holo-Grx4 and apo-SufA interact and to what degree they may form a stable complex, the two proteins were mixed together in anaerobic buffer containing 1 mM glutathione. When the SEC column was loaded with the mixture containing SufA and reconstituted Grx4, in a ~1:1 ratio, the results were that the mixture eluted as two overlapping peaks, with apparent MW of 27.8 kDa and 17.7 kDa (Table 2.1; Fig. 2.7, orange line). When comparing the higher MW peak of the mixture to the holo-Grx4 and as-purified SufA profiles, this elution peak correlated with neither the holo-Grx4 dimer nor the SufA dimer oligomer, eluting with a similar apparent molecular weight as the apo-Grx4/apo-SufA heterocomplex. It is possible that this elution profile demonstrates the existence of a natural intermediate complex between Grx4 and SufA, but the difference between homodimer vs. heterodimer profiles is negligible and below the resolution of the SEC column used. The lower MW peak of the mixture correlates with the monomeric elution peak of SufA and, in the gel, consists mainly of SufA. Comparison of chromatography results suggests that both apo- and holo-Grx4 form a heterodimeric complex with SufA (Figure 2.7). These data suggest that formation of a complex between Grx4 and SufA occurs regardless of the presence of the Fe−S cluster. The SDS-PAGE gel of holo-Grx4 / apo-SufA fractions (Fig. 2.7, bottom) shows that the higher MW peak is

composed of a mixture of both Grx4 and SufA as well as displaying protein bands in the ~35 kDa range. However, these fractions were also treated with trichloroacetic acid, which may have produced nonnative heterocomplex formation; so, the existence of this intermediate complex is uncertain. Each fraction was analyzed with CD spectroscopy to determine whether transfer of the iron-sulfur cluster from holo-Grx4 to apo-SufA occurred. Of the samples tested, the fraction corresponding to the upper MW peak produced a distinguishable signal (Fig. 2.8, blue line). The spectrum shows that there is a shallow positive peak in the 350-400 nm range in contrast to the broad negative peak in the holo-Grx4 spectrum (see Figure 2.4C). From what is known from the literature, holo-SufA has well-defined features in the visible region, including positive maxima at 350 and 465 nm and negative maxima at 317, 391, and 559 nm. The homodimer of SufA has no CD signal when the iron-sulfur cluster is absent from the active site. Therefore, the CD spectrum of the holo-Grx4 / apo-SufA mixture appears to have unique features that may indicate an intermediate complex has formed. When comparing the mixture CD spectrum to that of holo-Grx4 (see Fig. 2.4C, red line), a decrease in the 450 nm region in the presence of apo-SufA is observed, suggesting that the cluster may be partially transferred to apo-SufA However, since the spectrum baseline is shifted below the origin and the signal intensity is low, we cannot conclude that the spectrum demonstrates an accurate result.

Ni-NTA Affinity Chromatography to Characterize Protein-Protein Interactions Between His_6-Grx4 with Apo-SufA

Another approach to determine whether there is binding between holo-Grx4 and apo-SufA is to perform immobilized metal affinity chromatography (IMAC). Initially, reconstituted Grx4, containing an N-terminal polyhistidine tag (His_6-Grx4 in the

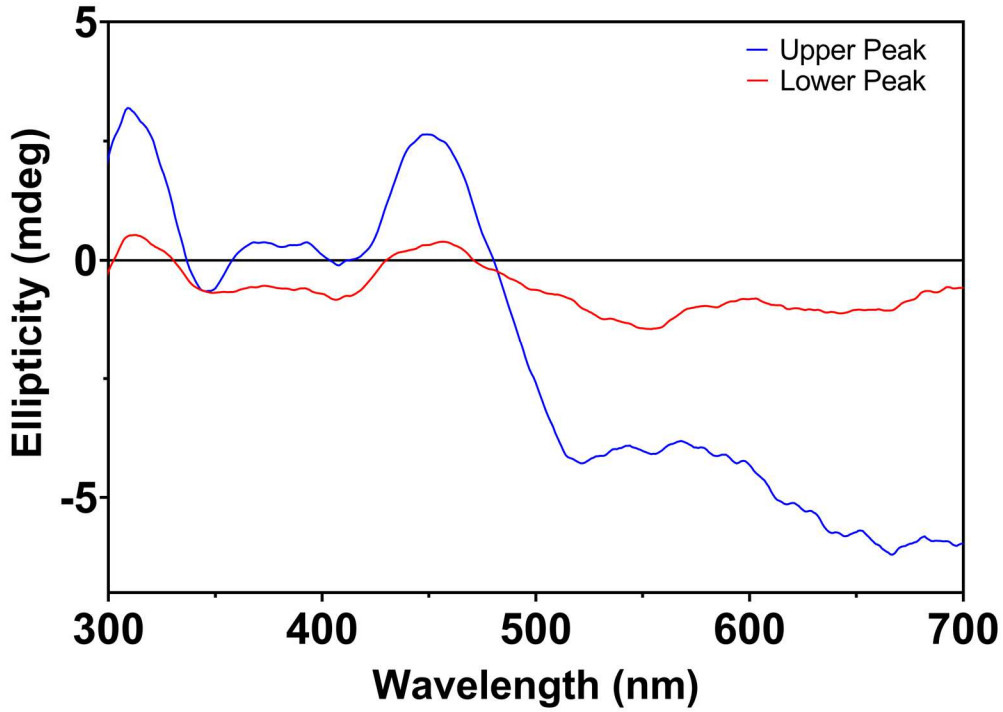

Figure 2.8. CD spectroscopy analysis of SEC Grx4−SufA Elution Fractions.

holo-form), was incubated with apo-SufA in an Eppendorf tube for 5 minutes before being loaded onto a Ni^{2+}-NTA column under anaerobic conditions. After a subsequent washing step, His_6-Grx4 and any proteins that interacted with it were eluted from the column using a high imidazole buffer. Secondly, this interaction experiment was repeated by performing sequential loading: reconstituted holo-His_6-Grx4 was bound to the Ni^{2+}-NTA column under anaerobic conditions. Apo-SufA was then passed through the preloaded His_6-Grx4 column under anaerobic conditions. After a brief incubation and subsequent washing step, His_6-Grx4 and any proteins that interacted with it were eluted from the column using a high imidazole buffer. The protein content of these elution fractions was analyzed by SDS-PAGE (Figure 2.9). As a control, apo-SufA was loaded, washed, and eluted on a Ni^{2+}-NTA column containing no His_6-Grx4 protein. Some non-specific SufA binding to the Ni^{2+}-NTA column was observed for these controls (not all SufA protein was found in the wash fractions). The interaction between apo-His_6-Grx4 and apo-SufA was also tested. The anaerobic interaction assay revealed that while holo-His_6-Grx4 does interact with apo-SufA (as observed in our SEC chromatography experiment), the apo-His_6-Grx4 / SufA interaction results did not differ significantly in the amount of apo-SufA that co-purified with His_6-Grx4, based on the two methods of testing. However, the Fe-S holo-Grx4 pre-incubated with apo-SufA maintained the reddish-brown protein complex coloration, characteristic of Fe-S cluster presence, throughout the column interaction experiment and the subsequent step of elution sample concentration. The stepwise loading of holo-His_6-Grx4 and apo-SufA also resulted in SufA and His_6-Grx4 co-eluting, but as a colorless protein solution. Although apo-SufA did seem to experience minimal non-specific binding to the Ni^{2+}-NTA column (Fig. 2.9), there was evidence of moderate protein-protein

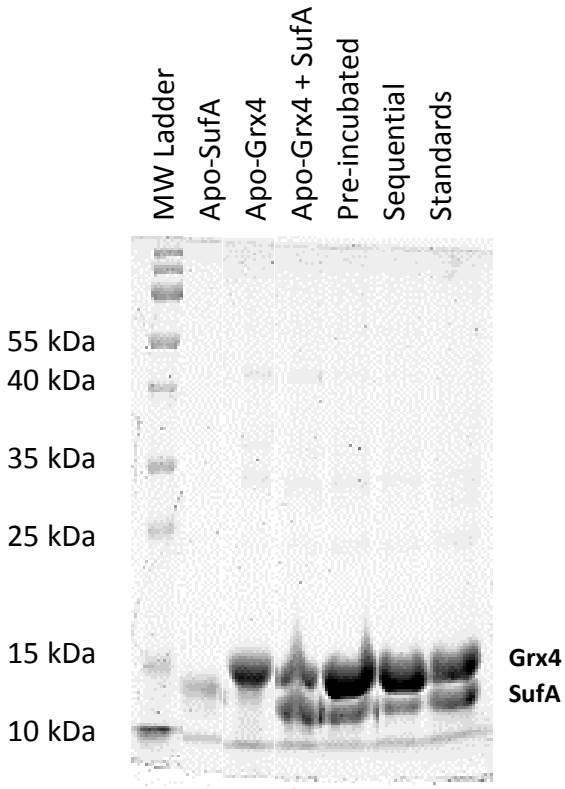

Figure 2.9. SufA interaction with apo- and Fe-S holo-forms of His-Grx4. Equal volumes of the elution fractions were analyzed for protein content by SDS-PAGE.

interaction between apo-His_6-Grx4 and apo-SufA (Fig. 2.9), when the proteins were pre-incubated before column loading. These results suggest that a linear model of Fe-S cluster assembly occurs, where cluster formation occurs first on the Grx4 followed by recruitment of apo-SufA, and unidirectional Fe-S cluster transfer to the SufA Fe-S shuttle.

In Vitro Cluster Transfer From [2Fe-2S] Cluster-Bound Grx4 to Apo-SufA

As previously mentioned, the intensity and superb sensitivity of the UV-visible CD spectra to the asymmetrical environment of biological [2Fe-2S] clusters has made CD spectroscopy the method of choice for monitoring the progress of interprotein Fe-S cluster transfer. The [2Fe-2S] center on monothiol Grx4 investigated in this work has distinct and intense UV-visible CD spectra compared to the [2Fe-2S] clusters on SufA (see Figure 2.4C). UV-visible CD spectra with Δε values were quantified based on the Fe-S cluster concentrations to provide a convenient method for quantitatively monitoring cluster transfer reactions based on changes in the Δε values at select wavelengths. As such, UV-visible CD spectroscopy was used to monitor changes in the Fe−S cluster coordination environment upon titration of holo-Grx4 with apo-SufA (Figure 2.10). The addition of an increasing number of equivalents of SufA resulted in the loss of the [2Fe-2S] Grx4 homodimer spectrum and formation of a weak spectrum that resembles that of a [2Fe-2S] Grx4−SufA heterodimer (see Figure 2.8). The transfer reaction reached equilibrium very quickly (< 5 min), before the first CD spectrum was recorded. These results suggest that titration of SufA with the [2Fe-2S] Grx4 homodimer promotes formation of a [2Fe-2S] Grx4−SufA heterodimer as well as that of the apo-Grx4/SufA heterodimer. However, given the shape of the apo-heterodimer peak in the chromatogram (see Figure 2.7, purple line) and the weaker [2Fe-2S] CD signal after addition of SufA (Figure 2.10), it appears

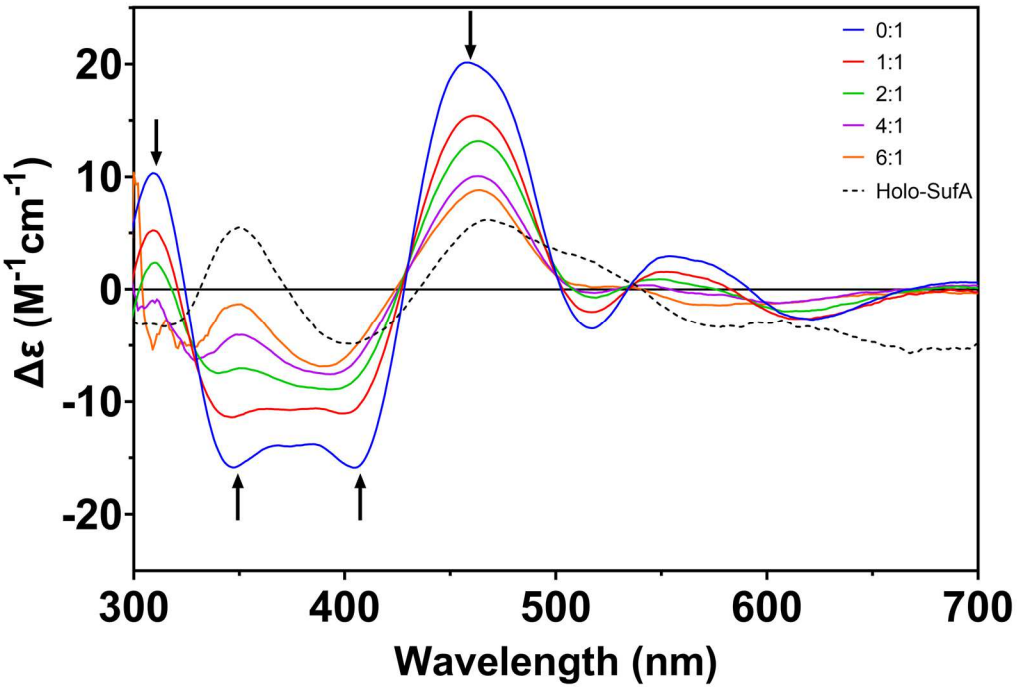

Figure 2.10. CD spectroscopy analysis of Grx4−SufA interactions. Titration study of the [2Fe-2S] Grx4 homodimer with apo-SufA monitored by UV−visible CD spectroscopy. CD spectra for the [2Fe-2S] cluster-bound Grx4 homodimer (blue line) titrated with a 0−6-fold excess of SufA (the legend indicates the SufA:[2Fe-2S] ratio). The arrows at selected wavelengths indicate the direction of the change in intensity with an increase in SufA concentration. Δε values are based on the initial [2Fe-2S] concentration, 100 μM.

that the majority of the Grx4−SufA heterodimer is isolated in the apo-form. Taken together with the SEC chromatogram, these results suggest that the interaction between Grx4 and SufA is not Fe−S cluster-dependent, and that SufA destabilizes the [2Fe-2S] cluster on Grx4 as it binds to form a stable intermediate heterocomplex. As a control, holo-SufA was anaerobically incubated with apo-Grx4 to determine whether the transfer reaction is bi-directional. The cluster transfer seems unidirectional, as the reverse reaction involving a 2:1 concentration of [2Fe-2S] cluster-bound SufA and monomeric apo-Grx4, in the presence of 1 mM GSH, showed no discernable change in the CD spectrum after 30 min of reaction monitoring (data not shown).

DISCUSSION

To clarify the nature of Grx4-SufA interactions in *E. coli*, we have purified Grx4 and SufA and characterized Fe-S cluster transfer interactions between them. Overall, the apparent molecular weights of the SufA homodimer, SufA-Grx4 complexes, and Grx4 homodimer, as determined by size-exclusion chromatography, were somewhat larger than the theoretical molecular weights of the homodimers and heterodimers. The monomer forms of SufA and Grx4 also ran slightly larger than their calculated molecular weights (see Table 2.1). Co-eluting samples of SufA and Grx4 separated into two resolved bands when subjected to reducing SDS-PAGE, indicating that the interaction between SufA and Grx4 may involve a covalent, intermolecular disulfide bond. As shown in Figure 2.4, fully reconstituted [2Fe-2S] forms of Grx4 and SufA have distinct CD absorption spectra from 300-700 nm. When holo-Grx4 is mixed with apo-SufA, we observe rapid Fe-S cluster transfer to SufA, as demonstrated by the loss of holo-Grx4 features and the appearance of CD features more similar to holo-SufA (Figure 10). In contrast, when holo-SufA was

mixed with apo-Grx4, cluster transfer was not observed, at least at the ratio tested. These results indicate that Fe-S cluster trafficking is unidirectional from *E. coli* Grx4 to SufA. Our preliminary results suggest that Grx4 may be able to load Fe-S clusters in SufA *in vivo*.

Although the gel filtration and CD interaction studies indicate that a Fe-S cluster transfer reaction is occurring between Grx4 and SufA, an alternate explanation for these results is that the data represents the CD spectrum of holo-Grx4 as its Fe-S cluster is destabilized from the active site over time by the presence of apo-SufA. Transfer of the Fe-S cluster from Grx4 to SufA is anticipated to occur in the order of seconds, so to track the protein-protein interaction, the kinetics of the reaction will need to be monitored over time using the CD spectrometer to determine whether transfer is occurring. In the simplest interaction model, the apo-SufA homodimer binds to holo-Grx4 to form a holo-Grx4 / apo-SufA heterodimer with a [2Fe-2S] bridging the two proteins (Figure 2.11). We hypothesize that the proteins come into contact and form a loosely associated protein–protein conformation that then either forms specific, close-range interactions in a native complex, or may remain kinetically trapped in a nonnative state, forming a heterocomplex intermediate, as a consequence of *in vitro* experimental conditions.

In vitro Fe-S cluster transfer experiments on the plant homologues of Grx4 and SufA revealed rapid, unidirectional, and intact cluster transfer from *A. thaliana* GrxS14 to *A. thaliana* SufA1.[62] Given that evidence shows that monothiol Grxs exist in cluster-bound forms *in vivo* in the cytosol of yeast,[103] and that monothiol Grxs and A-type proteins interact *in vivo* in yeast mitochondria,[75,83] it seems likely that rapid [2Fe-2S] cluster transfer from monothiol Grxs to A-type proteins, such as *E. coli* Grx4 and SufA, is a physiologically relevant cluster transfer reaction. Interestingly, previous studies have

shown the GSH molecules in Fe−S-bridged Grx homodimers are in dynamic equilibrium with GSH in solution.[104] This labile GSH coordination may allow access to the Fe−S cluster by competing ligands from SufA, facilitating formation of the heterodimer intermediate. Coupled with *in vivo* evidence for interaction between monothiol Grxs and A-type Fe–S cluster carrier proteins, the *in vitro* results from homologous proteins indicate that these two classes of proteins work together in cellular Fe–S cluster trafficking.

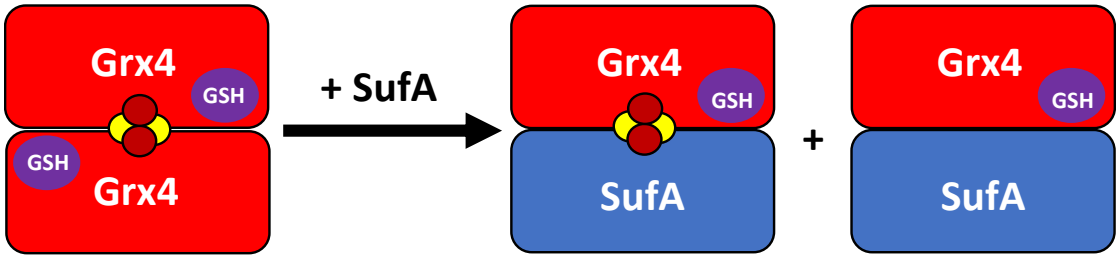

Figure 2.11. Model of interaction between the [2Fe-2S] Grx4 homodimer and SufA to form apo- and holo-Grx4−SufA heterodimers.

REFERENCES

1. Anbar, A.D., Duan, Y., Lyons, T.W., Arnold, G.L., Kendall, B., Creaser, R.A., Kaufman, A.J., Gordon, G.W., Scott, C., Garvin, J., and Buick, R. (2007). A Whiff of Oxygen Before the Great Oxidation Event? Science *317*, 1903-1906. 10.1126/science.1140325.

2. Anbar, A.D. (2008). OCEANS: Elements and Evolution. Science *322*, 1481-1483. 10.1126/science.1163100.

3. Konhauser, K.O., Pecoits, E., Lalonde, S.V., Papineau, D., Nisbet, E.G., Barley, M.E., Arndt, N.T., Zahnle, K., and Kamber, B.S. (2009). Oceanic nickel depletion and a methanogen famine before the Great Oxidation Event. Nature *458*, 750-753. 10.1038/nature07858.

4. Abbaspour, N., Hurrell, R., and Kelishadi, R. (2014). Review on iron and its importance for human health. Journal of Research in Medical Sciences *19*, 164-174.

5. Ilbert, M., and Bonnefoy, V. (2013). Insight into the evolution of the iron oxidation pathways. Biochimica et Biophysica Acta (BBA) - Bioenergetics *1827*, 161-175. 10.1016/j.bbabio.2012.10.001.

6. Lu, J.-B., Jian, J., Huang, W., Lin, H., Li, J., and Zhou, M. (2016). Experimental and theoretical identification of the Fe(vii) oxidation state in FeO^{4-}. Physical Chemistry Chemical Physics *18*, 31125-31131. 10.1039/c6cp06753k.

7. Scott, C., Lyons, T.W., Bekker, A., Shen, Y., Poulton, S.W., Chu, X., and Anbar, A.D. (2008). Tracing the stepwise oxygenation of the Proterozoic ocean. Nature *452*, 456-459. 10.1038/nature06811.

8. Andrews, S.C., Robinson, A.K., and Rodríguez-Quiñones, F. (2003). Bacterial iron homeostasis. FEMS Microbiology Reviews *27*, 215-237. 10.1016/s0168-6445(03)00055-x.

9. Imlay, J.A., Chin, S.M., and Linn, S. (1988). Toxic DNA Damage By Hydrogen-Peroxide Through The Fenton Reaction *In vivo* And *In vitro*. Science *240*, 640-642. 10.1126/science.2834821.

10. Ratledge, C., and Dover, L.G. (2000). Iron Metabolism in Pathogenic Bacteria. Annual Review of Microbiology *54*, 881-941. 10.1146/annurev.micro.54.1.881.

11. Reiter, R.J., Melchiorri, D., Sewerynek, E., Poeggeler, B., Barlowwalden, L., Chuang, J.I., Ortiz, G.G., and Acunacastroviejo, D. (1995). A Review Of The Evidence Supporting Melatonins Role As An Antioxidant. Journal of Pineal Research *18*, 1-11. 10.1111/j.1600-079X.1995.tb00133.x.

12. Winterbourn, C.C. (1995). Toxicity of iron and hydrogen peroxide: the Fenton reaction. Toxicology Letters *82-83*, 969-974. 10.1016/0378-4274(95)03532-x.

13. Przybyla-Toscano, J., Roland, M., Gaymard, F., Couturier, J., and Rouhier, N. (2018). Roles and maturation of iron–sulfur proteins in plastids. JBIC Journal of Biological Inorganic Chemistry *23*, 545-566. 10.1007/s00775-018-1532-1.

14. Huber, C. (2003). A Possible Primordial Peptide Cycle. Science *301*, 938-940. 10.1126/science.1086501.

15. Wächtershäuser, G. (2007). On the Chemistry and Evolution of the Pioneer Organism. Chemistry & Biodiversity *4*, 584-602. 10.1002/cbdv.200790052.

16. Bandyopadhyay, S., Chandramouli, K., and Johnson, M.K. (2008). Iron-sulfur cluster biosynthesis. Biochemical Society Transactions *36*, 1112-1119. 10.1042/bst0361112.

17. Rouault, T.A. (2019). The indispensable role of mammalian iron sulfur proteins in function and regulation of multiple diverse metabolic pathways. BioMetals *32*, 343-353. 10.1007/s10534-019-00191-7.

18. Ribbe, M.W., Hu, Y., Hodgson, K.O., and Hedman, B. (2014). Biosynthesis of Nitrogenase Metalloclusters. Chemical Reviews *114*, 4063-4080. 10.1021/cr400463x.

19. Fontecave, M. (2006). Iron-sulfur clusters: ever-expanding roles. Nature Chemical Biology *2*, 171-174. 10.1038/nchembio0406-171.

20. Roche, B., Aussel, L., Ezraty, B., Mandin, P., Py, B., and Barras, F. (2013). Iron/sulfur proteins biogenesis in prokaryotes: Formation, regulation and diversity. Biochimica et Biophysica Acta (BBA) - Bioenergetics *1827*, 455-469. 10.1016/j.bbabio.2012.12.010.

21. Johnson, D.C., Dean, D.R., Smith, A.D., and Johnson, M.K. (2005). Structure, function, and formation of biological iron-sulfur clusters. Annual Review of Biochemistry *74*, 247-281. 10.1146/annurev.biochem.74.082803.133518.

22. Johnson, M.K. (1998). Iron-sulfur proteins: new roles for old clusters. Current Opinion in Chemical Biology *2*, 173-181. 10.1016/s1367-5931(98)80058-6.

23. Demple, B., Ding, H.E., and Jorgensen, M. (2002). *Escherichia coli* SoxR protein: Sensor/transducer of oxidative stress and nitric oxide. Protein Sensors and Reactive Oxygen Species, Pt B, Thiol Enzymes and Proteins *348*, 355-364. 10.1016/s0076-6879(02)48654-5.

24. Brancaccio, D., Gallo, A., Piccioli, M., Novellino, E., Ciofi-Baffoni, S., and Banci, L. (2017). [4Fe-4S] Cluster Assembly in Mitochondria and Its Impairment by Copper. Journal of the American Chemical Society *139*, 719-730. 10.1021/jacs.6b09567.

25. Garcia-Santamarina, S., Uzarska, M.A., Festa, R.A., Lill, R., and Thiele, D.J. (2017). Cryptococcus neoformans Iron-Sulfur Protein Biogenesis Machinery Is a Novel Layer of Protection against Cu Stress. mBio *8*. 10.1128/mbio.01742-17.

26. Sheftel, A., Stehling, O., and Lill, R. (2010). Iron-sulfur proteins in health and disease. Trends in Endocrinology and Metabolism *21*, 302-314. 10.1016/j.tem.2009.12.006.

27. Rouault, T.A. (2012). Biogenesis of iron-sulfur clusters in mammalian cells: new insights and relevance to human disease. Disease Models & Mechanisms *5*, 155-164. 10.1242/dmm.009019.

28. Wachnowsky, C., Fidai, I., and Cowan, J.A. (2018). Iron-sulfur cluster biosynthesis and trafficking - impact on human disease conditions. Metallomics *10*, 9-29. 10.1039/c7mt00180k.

29. Tsaousis, A.D. (2019). On the Origin of Iron/Sulfur Cluster Biosynthesis in Eukaryotes. Frontiers in Microbiology *10*, 10, 2478. 10.3389/fmicb.2019.02478.

30. Cupp-Vickery, J.R., Urbina, H., and Vickery, L.E. (2003). Crystal structure of IscS, a cysteine desulfurase from *Escherichia coli*. Journal of Molecular Biology *330*, 1049-1059. 10.1016/s0022-2836(03)00690-9.

31. Outten, F.W. (2015). Recent advances in the Suf Fe-S cluster biogenesis pathway: Beyond the Proteobacteria. Biochimica Et Biophysica Acta-Molecular Cell Research *1853*, 1464-1469. 10.1016/j.bbamcr.2014.11.001.

32. Vinella, D., Brochier-Armanet, C., Loiseau, L., Talla, E., and Barras, F. (2009). Iron-Sulfur (Fe/S) Protein Biogenesis: Phylogenomic and Genetic Studies of A-Type Carriers. Plos Genetics *5*, e1000497. 10.1371/journal.pgen.1000497.

33. Blanc, B., Gerez, C., and de Choudens, S.A. (2015). Assembly of Fe/S proteins in bacterial systems Biochemistry of the bacterial ISC system. Biochimica Et Biophysica Acta-Molecular Cell Research *1853*, 1436-1447. 10.1016/j.bbamcr.2014.12.009.

34. Mapolelo, D.T., Zhang, B., Naik, S.G., Huynh, B.H., and Johnson, M.K. (2012). Spectroscopic and Functional Characterization of Iron–Sulfur Cluster-Bound Forms of Azotobacter vinelandiiNifIscA. Biochemistry *51*, 8071-8084. 10.1021/bi3006658.

35. Beilschmidt, L.K., and Puccio, H.M. (2014). Mammalian Fe-S cluster biogenesis and its implication in disease. Biochimie *100*, 48-60. 10.1016/j.biochi.2014.01.009.

36. Giel, J.L., Nesbit, A.D., Mettert, E.L., Fleischhacker, A.S., Wanta, B.T., and Kiley, P.J. (2013). Regulation of iron-sulphur cluster homeostasis through transcriptional control of the Isc pathway by [2Fe-2S]-IscR inEscherichia coli. Molecular Microbiology *87*, 478-492. 10.1111/mmi.12052.

37. Agar, J.N., Krebs, C., Frazzon, J., Huynh, B.H., Dean, D.R., and Johnson, M.K. (2000). IscU as a Scaffold for Iron−Sulfur Cluster Biosynthesis: Sequential Assembly of [2Fe-2S] and [4Fe-4S] Clusters in IscU. Biochemistry *39*, 7856-7862. 10.1021/bi000931n.

38. Kato, S.-I., Mihara, H., Kurihara, T., Takahashi, Y., Tokumoto, U., Yoshimura, T., and Esaki, N. (2002). Cys-328 of IscS and Cys-63 of IscU are the sites of disulfide bridge formation in a covalently bound IscS/IscU complex: Implications for the mechanism of iron-sulfur cluster assembly. Proceedings of the National Academy of Sciences *99*, 5948-5952. 10.1073/pnas.082123599.

39. Ollagnier-de-Choudens, S., Sanakis, Y., and Fontecave, M. (2004). SufA/IscA: reactivity studies of a class of scaffold proteins involved in Fe-S cluster assembly. Journal of Biological Inorganic Chemistry *9*, 828-838. 10.1007/s00775-004-0581-9.

40. Bonomi, F., Iametti, S., Morleo, A., Ta, D., and Vickery, L.E. (2008). Studies on the Mechanism of Catalysis of Iron−Sulfur Cluster Transfer from IscU[2Fe2S] by HscA/HscB Chaperones. Biochemistry *47*, 12795-12801. 10.1021/bi801565j.

41. Kim, J.H., Füzéry, A.K., Tonelli, M., Ta, D.T., Westler, W.M., Vickery, L.E., and Markley, J.L. (2009). Structure and Dynamics of the Iron−Sulfur Cluster Assembly Scaffold Protein IscU and Its Interaction with the Cochaperone HscB. Biochemistry *48*, 6062-6071. 10.1021/bi9002277.

42. Chandramouli, K., and Johnson, M.K. (2006). HscA and HscB Stimulate [2Fe-2S] Cluster Transfer from IscU to Apoferredoxin in an ATP-Dependent Reaction. Biochemistry *45*, 11087-11095. 10.1021/bi061237w.

43. Chahal, H.K., and Outten, F.W. (2012). Separate Fe - S scaffold and carrier functions for SufB(2)C(2) and SufA during in vitro maturation of 2Fe-2S Fdx. Journal of Inorganic Biochemistry *116*, 126-134. 10.1016/j.jinorgbio.2012.06.008.

44. Shimomura, Y., Takahashi, Y., Kakuta, Y., and Fukuyama, K. (2005). Crystal structure of Escherichia coli YfhJ protein, a member of the ISC machinery involved in assembly of iron-sulfur clusters. Proteins: Structure, Function, and Bioinformatics *60*, 566-569. 10.1002/prot.20481.

45. Pastore, C., Adinolfi, S., Huynen, M.A., Rybin, V., Martin, S., Mayer, M., Bukau, B., and Pastore, A. (2006). YfhJ, a Molecular Adaptor in Iron-Sulfur Cluster Formation or a Frataxin-like Protein? Structure *14*, 857-867. 10.1016/j.str.2006.02.010.

46. Kim, J.H., Bothe, J.R., Frederick, R.O., Holder, J.C., and Markley, J.L. (2014). Role of IscX in Iron–Sulfur Cluster Biogenesis in Escherichia coli. Journal of the American Chemical Society *136*, 7933-7942. 10.1021/ja501260h.

47. Ren, X.J., Liang, F., He, Z.F., Fan, B.Q., Zhang, Z.R., Guo, X.D., Du, Y.K., Pang, Y.L., Li, J.H., Lyu, J.X., and Tan, G.Q. (2021). Identification of an Intermediate Form of Ferredoxin That Binds Only Iron Suggests That Conversion to Holo-Ferredoxin Is Independent of the ISC System in Escherichia coli. Applied and Environmental Microbiology *87*, 16, e03153-20. 10.1128/aem.03153-20.

48. Fontecave, M., and Ollagnier-De-Choudens, S. (2008). Iron-sulfur cluster biosynthesis in bacteria: Mechanisms of cluster assembly and transfer. Archives of Biochemistry and Biophysics *474*, 226-237. 10.1016/j.abb.2007.12.014.

49. Dai, Y., and Outten, F.W. (2012). TheE. coliSufS-SufE sulfur transfer system is more resistant to oxidative stress than IscS-IscU. FEBS Letters *586*, 4016-4022. 10.1016/j.febslet.2012.10.001.

50. Selbach, B.P., Pradhan, P.K., and Dos Santos, P.C. (2013). Protected Sulfur Transfer Reactions by the Escherichia coli Suf System. Biochemistry *52*, 4089-4096. 10.1021/bi4001479.

51. Outten, F.W., Wood, M.J., Munoz, F.M., and Storz, G. (2003). The SufE protein and the SufBCD complex enhance SufS cysteine desulfurase activity as part of a sulfur transfer pathway for fe-s cluster assembly in Escherichia coli. Journal of Biological Chemistry *278*, 45713-45719. 10.1074/jbc.M308004200.

52. Garcia, P.S., Gribaldo, S., Py, B., and Barras, F. (2019). The SUF system: an ABC ATPase-dependent protein complex with a role in Fe-S cluster biogenesis. Research in Microbiology *170*, 426-434. 10.1016/j.resmic.2019.08.001.

53. Blanc, B., Clemancey, M., Latour, J.M., Fontecave, M., and de Choudens, S.O. (2014). Molecular Investigation of Iron Sulfur Cluster Assembly Scaffolds under Stress. Biochemistry *53*, 7867-7869. 10.1021/bi5012496.

54. Yuda, E., Tanaka, N., Fujishiro, T., Yokoyama, N., Hirabayashi, K., Fukuyama, K., Wada, K., and Takahashi, Y. (2017). Mapping the key residues of SufB and SufD essential for biosynthesis of iron-sulfur clusters. Scientific Reports *7*, 9387. 10.1038/s41598-017-09846-2.

55. Hirabayashi, K., Yuda, E., Tanaka, N., Katayama, S., Iwasaki, K., Matsumoto, T., Kurisu, G., Outten, F.W., Fukuyama, K., Takahashi, Y., and Wada, K. (2015). Functional Dynamics Revealed by the Structure of the SufBCD Complex, a Novel ATP-binding Cassette (ABC) Protein That Serves as a Scaffold for Iron-Sulfur Cluster Biogenesis. Journal of Biological Chemistry *290*, 29717-29731. 10.1074/jbc.M115.680934.

56. Saini, A., Mapolelo, D.T., Chahal, H.K., Johnson, M.K., and Outten, F.W. (2010). SufD and SufC ATPase Activity Are Required for Iron Acquisition during in Vivo Fe-S Cluster Formation on SufB. Biochemistry *49*, 9402-9412. 10.1021/bi1011546.

57. Chahal, H.K., Dai, Y.Y., Saini, A., Ayala-Castro, C., and Outten, F.W. (2009). The SufBCD Fe-S Scaffold Complex Interacts with SufA for Fe-S Cluster Transfer. Biochemistry *48*, 10644-10653. 10.1021/bi901518y.

58. Ollagnier-de Choudens, S., Nachin, L., Sanakis, Y., Loiseau, L., Barras, F., and Fontecave, M. (2003). SufA from Erwinia chrysanthemi - Characterization of a scaffold protein required for iron-sulfur cluster assembly. Journal of Biological Chemistry *278*, 17993-18001. 10.1074/jbc.M300285200.

59. Loiseau, L., Gerez, C., Bekker, M., Choudens, S.O.D., Py, B., Sanakis, Y., de Mattos, J.T., Fontecave, M., and Barras, F. (2007). ErpA, an iron-sulfur (Fe-S) protein of the A-type essential for respiratory metabolism in Escherichia coli. Proceedings of the National Academy of Sciences of the United States of America *104*, 13626-13631. 10.1073/pnas.0705829104.

60. Gupta, V., Sendra, M., Naik, S.G., Chahal, H.K., Huynh, B.H., Outten, F.W., Fontecave, M., and de Choudens, S.O. (2009). Native Escherichia coli SufA, Coexpressed with SufBCDSE, Purifies as a 2Fe-2S Protein and Acts as an Fe-S Transporter to Fe-S Target Enzymes. Journal of the American Chemical Society *131*, 6149-6153. 10.1021/ja807551e.

61. Py, B., Gerez, C., Huguenot, A., Vidaud, C., Fontecave, M., de Choudens, S.O., and Barras, F. (2018). The ErpA/NfuA complex builds an oxidation-resistant Fe-S cluster delivery pathway. Journal of Biological Chemistry *293*, 7689-7702. 10.1074/jbc.RA118.002160.

62. Mapolelo, D.T., Zhang, B., Randeniya, S., Albetel, A.N., Li, H.R., Couturier, J., Outten, C.E., Rouhier, N., and Johnson, M.K. (2013). Monothiol glutaredoxins and A-type proteins: partners in Fe-S cluster trafficking. Dalton Transactions *42*, 3107-3115. 10.1039/c2dt32263c.

63. Landry, A.P., Cheng, Z., and Ding, H. (2013). Iron binding activity is essential for the function of IscA in iron–sulphur cluster biogenesis. Dalton Trans. *42*, 3100-3106. 10.1039/c2dt32000b.

64. Ding, B., Smith, S., Edward, and Ding, H. (2005). Mobilization of the iron centre in IscA for the iron–sulphur cluster assembly in IscU. Biochemical Journal *389*, 797-802. 10.1042/bj20050405.

65. Lu, J.X., Yang, J.J., Tan, G.Q., and Ding, H.G. (2008). Complementary roles of SufA and IscA in the biogenesis of iron-sulfur clusters in Escherichia coli. Biochemical Journal *409*, 535-543. 10.1042/bj20071166.

66. Vinella, D., Loiseau, L., de Choudens, S.O., Fontecave, M., and Barras, F. (2013). In vivo Fe-S cluster acquisition by IscR and NsrR, two stress regulators in Escherichia coli. Molecular Microbiology *87*, 493-508. 10.1111/mmi.12135.

67. Jensen, L.T., and Culotta, V.C. (2000). Role of Saccharomyces cerevisiae ISA1 and ISA2 in iron homeostasis. Molecular and Cellular Biology *20*, 3918-3927. 10.1128/mcb.20.11.3918-3927.2000.

68. Wada, K., Hasegawa, Y., Gong, Z., Minami, Y., Fukuyama, K., and Takahashi, Y. (2005). Crystal structure of Escherichia coli SufA involved in biosynthesis of iron-sulfur clusters: Implications for a functional dimer. Febs Letters *579*, 6543-6548. 10.1016/j.febslet.2005.10.046.

69. Fernandes, A.P., and Holmgren, A. (2004). Glutaredoxins: Glutathione-dependent redox enzymes with functions far beyond a simple thioredoxin backup system. Antioxidants & Redox Signaling *6*, 63-74. 10.1089/152308604771978354.

70. Fernandes, A.P., Fladvad, M., Berndt, C., Andresen, C., Lillig, C.H., Neubauer, P., Sunnerhagen, M., Holmgren, A., and Vlamis-Gardikas, A. (2005). A novel monothiol glutaredoxin (Grx4) from Escherichia coli can serve as a substrate for thioredoxin reductase. Journal of Biological Chemistry *280*, 24544-24552. 10.1074/jbc.M500678200.

71. Iwema, T., Picciocchi, A., Traore, D.A.K., Ferrer, J.-L., Chauvat, F., and Jacquamet, L. (2009). Structural Basis for Delivery of the Intact [Fe2S2] Cluster by Monothiol Glutaredoxin. Biochemistry *48*, 6041-6043. 10.1021/bi900440m.

72. Lillig, C.H., Berndt, C., and Holmgren, A. (2008). Glutaredoxin systems. Biochimica Et Biophysica Acta-General Subjects *1780*, 1304-1317. 10.1016/j.bbagen.2008.06.003.

73. RodríGuez-Manzaneque, M.T., Ros, J., Cabiscol, E., Sorribas, A., and Herrero, E. (1999). Grx5 Glutaredoxin Plays a Central Role in Protection against Protein Oxidative Damage in Saccharomyces cerevisiae. Molecular and Cellular Biology *19*, 8180-8190. 10.1128/mcb.19.12.8180.

74. Rodriguez-Manzaneque, M.T., Tamarit, J., Belli, G., Ros, J., and Herrero, E. (2002). Grx5 is a mitochondrial glutaredoxin required for the activity of iron/sulfur enzymes. Molecular Biology of the Cell *13*, 1109-1121. 10.1091/mbc.01-10-0517.

75. Vilella, F., Alves, R., Rodríguez-Manzaneque, M.T., Bellí, G., Swaminathan, S., Sunnerhagen, P., and Herrero, E. (2004). Evolution and Cellular Function of Monothiol Glutaredoxins: Involvement in Iron-Sulphur Cluster Assembly. Comparative and Functional Genomics *5*, 328-341. 10.1002/cfg.406.

76. Yeung, N., Gold, B., Liu, N.L., Prathapam, R., Sterling, H.J., Willams, E.R., and Butland, G. (2011). The E. coli Monothiol Glutaredoxin GrxD Forms Homodimeric and Heterodimeric FeS Cluster Containing Complexes. Biochemistry *50*, 8957-8969. 10.1021/bi2008883.

77. Butland, G., Babu, M., Diaz-Mejia, J.J., Bohdana, F., Phanse, S., Gold, B., Yang, W.H., Li, J., Gagarinova, A.G., Pogoutse, O., et al. (2008). eSGA: E. coli synthetic genetic array analysis. Nature Methods *5*, 789-795. 10.1038/nmeth.1239.

78. Boutigny, S., Saini, A., Baidoo, E.E.K., Yeung, N., Keasling, J.D., and Butland, G. (2013). Physical and Functional Interactions of a Monothiol Glutaredoxin and an Iron Sulfur Cluster Carrier Protein with the Sulfur-donating Radical S-Adenosyl-l-methionine Enzyme MiaB. Journal of Biological Chemistry *288*, 14200-14211. 10.1074/jbc.m113.460360.

79. Riboldi, G.P., de Oliveira, J.S., and Frazzon, J. (2011). Enterococcus faecalis SufU scaffold protein enhances SufS desulfurase activity by acquiring sulfur from its cysteine-153. Biochimica Et Biophysica Acta-Proteins and Proteomics *1814*, 1910-1918. 10.1016/j.bbapap.2011.06.016.

80. Huet, G.L., Daffé, M., and Saves, I. (2005). Identification of the Mycobacterium tuberculosis SUF Machinery as the Exclusive Mycobacterial System of [Fe-S] Cluster Assembly: Evidence for Its Implication in the Pathogen's Survival. Journal of Bacteriology *187*, 6137-6146. 10.1128/jb.187.17.6137-6146.2005.

81. Herb, M., and Schramm, M. (2021). Functions of ROS in Macrophages and Antimicrobial Immunity. Antioxidants *10*, 313. 10.3390/antiox10020313.

82. Muhlenhoff, U., Gerber, J., Richhardt, N., and Lill, R. (2003). Components involved in assembly and dislocation of iron-sulfur clusters on the scaffold protein Isu1p. Embo Journal *22*, 4815-4825. 10.1093/emboj/cdg446.

83. Kim, K.D., Chung, W.H., Kim, H.J., Lee, K.C., and Roe, J.H. (2010). Monothiol glutaredoxin Grx5 interacts with Fe-S scaffold proteins Isa1 and Isa2 and supports Fe-S assembly and DNA integrity in mitochondria of fission yeast. Biochemical and Biophysical Research Communications *392*, 467-472. 10.1016/j.bbrc.2010.01.051.

84. Belli, G., Polaina, J., Tamarit, J., de la Torre, M.A., Rodriguez-Manzaneque, M.T., Ros, J., and Herrero, E. (2002). Structure-function analysis of yeast Grx5 monothiol glutaredoxin defines essential amino acids for the function of the protein. Journal of Biological Chemistry *277*, 37590-37596. 10.1074/jbc.M201688200.

85. Herrero, E., and de la Torre-Ruiz, M.A. (2007). Monothiol glutaredoxins: a common domain for multiple functions. Cellular and Molecular Life Sciences *64*, 1518-1530. 10.1007/s00018-007-6554-8.

86. Li, H.R., and Outten, C.E. (2012). Monothiol CGFS Glutaredoxins and BolA-like Proteins: 2Fe-2S Binding Partners in Iron Homeostasis. Biochemistry *51*, 4377-4389. 10.1021/bi300393z.

87. Li, H., Mapolelo, D.T., Dingra, N.N., Naik, S.G., Lees, N.S., Hoffman, B.M., Riggs-Gelasco, P.J., Huynh, B.H., Johnson, M.K., and Outten, C.E. (2009). The Yeast Iron Regulatory Proteins Grx3/4 and Fra2 Form Heterodimeric Complexes Containing a [2Fe-2S] Cluster with Cysteinyl and Histidyl Ligation. Biochemistry *48*, 9569-9581. 10.1021/bi901182w.

88. Dlouhy, A.C., Beaudoin, J., Labbé, S., and Outten, C.E. (2017). Schizosaccharomyces pombe Grx4 regulates the transcriptional repressor Php4 via [2Fe–2S] cluster binding. Metallomics *9*, 1096-1105. 10.1039/c7mt00144d.

89. Zhang, B., Bandyopadhyay, S., Shakamuri, P., Naik, S.G., Huynh, B.H., Couturier, J., Rouhier, N., and Johnson, M.K. (2013). Monothiol Glutaredoxins Can Bind Linear [Fe3S4]+ and [Fe4S4]2+ Clusters in Addition to [Fe2S2]2+ Clusters: Spectroscopic Characterization and Functional Implications. Journal of the American Chemical Society *135*, 15153-15164. 10.1021/ja407059n.

90. Vranish, J.N., Das, D., and Barondeau, D.P. (2016). Real-Time Kinetic Probes Support Monothiol Glutaredoxins As Intermediate Carriers in Fe-S Cluster Biosynthetic Pathways. Acs Chemical Biology *11*, 3114-3121. 10.1021/acschembio.6b00632.

91. Butland, G., Peregrín-Alvarez, J.M., Li, J., Yang, W., Yang, X., Canadien, V., Starostine, A., Richards, D., Beattie, B., Krogan, N., et al. (2005). Interaction network containing conserved and essential protein complexes in Escherichia coli. Nature *433*, 531-537. 10.1038/nature03239.

92. Kennedy, M.C., and Beinert, H. (1988). The state of cluster SH and S2- of aconitase during cluster interconversions and removal. A convenient preparation of apoenzyme. Journal of Biological Chemistry *263*, 8194-8198. 10.1016/s0021-9258(18)68461-3.

93. Riemer, J., Hoepken, H.H., Czerwinska, H., Robinson, S.R., and Dringen, R. (2004). Colorimetric ferrozine-based assay for the quantitation of iron in cultured cells. Analytical Biochemistry *331*, 370-375. 10.1016/j.ab.2004.03.049.

94. Broderick, J.B., Henshaw, T.F., Cheek, J., Wojtuszewski, K., Smith, S.R., Trojan, M.R., Mcghan, R.M., Kopf, A., Kibbey, M., and Broderick, W.E. (2000). Pyruvate Formate-Lyase-Activating Enzyme: Strictly Anaerobic Isolation Yields Active Enzyme Containing a [3Fe–4S]+ Cluster. Biochemical and Biophysical Research Communications *269*, 451-456. 10.1006/bbrc.2000.2313.

95. Beinert, H. (1983). Semi-Micro Methods For Analysis Of Labile Sulfide And Of Labile Sulfide Plus Sulfane Sulfur In Unusually Stable Iron Sulfur Proteins. Analytical Biochemistry *131*, 373-378. 10.1016/0003-2697(83)90186-0.

96. Krebs, C., Agar, J.N., Smith, A.D., Frazzon, J., Dean, D.R., Huynh, B.H., and Johnson, M.K. (2001). IscA, an alternate scaffold for Fe-S cluster biosynthesis. Biochemistry *40*, 14069-14080. 10.1021/bi015656z.

97. Morimoto, K., Nishio, K., and Nakai, M. (2002). Identification of a novel prokaryotic HEAT-repeats-containing protein which interacts with a cyanobacterial IscA homolog. FEBS Letters *519*, 123-127. 10.1016/s0014-5793(02)02736-9.

98. Wollenberg, M., Berndt, C., Bill, E., Schwenn, J.D., and Seidler, A. (2003). A dimer of the FeS cluster biosynthesis protein IscA from cyanobacteria binds a [2Fe2S] cluster between two protomers and transfers it to [2Fe2S] and [4Fe4S] apo proteins. European Journal of Biochemistry *270*, 1662-1671. 10.1046/j.1432-1033.2003.03522.x.

99. Wu, G., Mansy, S.S., Hemann, C., Hille, R., Surerus, K.K., and Cowan, J. (2002). Iron-sulfur cluster biosynthesis: characterization of Schizosaccharomyces pombe Isa1. JBIC Journal of Biological Inorganic Chemistry *7*, 526-532. 10.1007/s00775-001-0330-2.

100. Ollagnier-De-Choudens, S., Mattioli, T., Takahashi, Y., and Fontecave, M. (2001). Iron-Sulfur Cluster Assembly. Journal of Biological Chemistry *276*, 22604-22607. 10.1074/jbc.m102902200.

101. Chahal, H.K., Dai, Y., Saini, A., Ayala-Castro, C., and Outten, F.W. (2009). The SufBCD Fe−S Scaffold Complex Interacts with SufA for Fe−S Cluster Transfer. Biochemistry *48*, 10644-10653. 10.1021/bi901518y.

102. Dlouhy, A.C., Li, H.R., Albetel, A.N., Zhang, B., Mapolelo, D.T., Randeniya, S., Holland, A.A., Johnson, M.K., and Outten, C.E. (2016). The Escherichia coli BolA Protein IbaG Forms a Histidine-Ligated 2Fe-2S -Bridged Complex with Grx4. Biochemistry *55*, 6869-6879. 10.1021/acs.biochem.6b00812.

103. Mühlenhoff, U., Molik, S., Godoy, J.R., Uzarska, M.A., Richter, N., Seubert, A., Zhang, Y., Stubbe, J., Pierrel, F., Herrero, E., et al. (2010). Cytosolic Monothiol Glutaredoxins Function in Intracellular Iron Sensing and Trafficking via Their Bound Iron-Sulfur Cluster. Cell Metabolism *12*, 373-385. 10.1016/j.cmet.2010.08.001.

104. Berndt, C., Hudemann, C., Hanschmann, E.M., Axelsson, R., Holmgren, A., and Lillig, C.H. (2007). How does iron-sulfur cluster coordination regulate the activity of human glutaredoxin 2? Antioxidants & Redox Signaling *9*, 151-157. 10.1089/ars.2007.9.151.